

Feasibility and Implementation of Balanced Mix Design in Nebraska

Gabriel Nsengiyumva, Yong-Rak Kim
Zachry Department of Civil and Environmental Engineering
Texas A&M University
College Station, Texas

and

Jiong Hu
Department of Civil and Environmental Engineering
University of Nebraska-Lincoln
Omaha, Nebraska

Sponsored by
Nebraska Department of Transportation and U.S. Department of
Transportation Federal Highway Administration

September 2020



Technical Report Documentation Page

1. Report No. SPR-P1(19) M080	2. Government Accession No.	3. Recipient's Catalog No.	
4. Title and Subtitle Feasibility and Implementation of Balanced Mix Design in Nebraska		5. Report Date September 15, 2020	
		6. Performing Organization Code	
7. Author(s) Gabriel Mukristu Nsengiyumva, Yong-Rak Kim, and Jiong Hu		8. Performing Organization Report No.	
9. Performing Organization Name and Address Prime Organization: Department of Civil and Environmental Engineering University of Nebraska-Lincoln Omaha, Nebraska 68182 Subaward Organization: Zachry Department of Civil and Environmental Engineering Texas A&M University College Station, Texas 77843-3136		10. Work Unit No.	
		11. Contract SPR-1(18) M070	
12. Sponsoring Agency Name and Address Nebraska Department of Transportation Research Section 1400 Hwy 2 Lincoln, NE 68502		13. Type of Report and Period Covered Final Report - Draft	
		14. Sponsoring Agency Code	
15. Supplementary Notes			
16. Abstract Balanced mixture design is an alternative asphalt concrete design method that incorporates the performance of mixtures during the design. Balanced mixture design consists of performance test methods and performance criteria. Compared to the existing Superpave design method which mostly relies on volumetrics to design mixtures, balanced mixture design is more suited to account for performance improvements originating from reclaimed asphalt pavement and other foreign additives such as rejuvenators, warm-mix asphalt additives, polymers, and anti-stripping agents. This study investigated the feasibility of the implementation of balanced mixture design in Nebraska mixtures by exploring appropriate test methods (i.e., for fracture and rutting) and method of selection of performance criteria. For the fracture test, the semicircular bend test method was selected and investigated for the appropriate testing conditions that can provide repeatable results. These testing conditions included: the number of replicates, specimen thickness, testing temperature, notch length, and loading rate. Also, the effect of the semicircular bend testing configurations on the test results and their repeatability was explored. For the rutting performance test, a simple rutting test called Gyratory stability was explored by determining critical testing conditions that can aid repeatable results and practical implementation. The validity of the newly developed Gyratory stability test was accomplished by correlating its test results to that of the established flow number test. The correlation showed interchangeability between the Gyratory stability and the flow number, which demonstrated the feasibility of the Gyratory stability as a rutting performance test. Finally, the two performance tests (semicircular bending and Gyratory stability) were conducted for typical Nebraska asphalt concrete mixtures and several additional mixtures including high amounts of recycled materials with rejuvenating agents. Test results were incorporated with a performance space diagram.			
17. Key Words Asphalt Concrete Mixture, Balanced Mix Design, Cracking, Rutting, Performance Space Diagram		18. Distribution Statement No restrictions. This document is available through the National Technical Information Service. 5285 Port Royal Road Springfield, VA 22161	
19. Security Classification (of this report) Unclassified	20. Security Classification (of this page) Unclassified	21. No. of Pages 92	22. Price

Table of Contents

Technical Report Documentation Page	ii
List of Figures	v
List of Tables	viii
Acknowledgment	ix
Disclaimer	x
Abstract	xi
Chapter 1 Introduction.....	1
1.1 Research Objective	5
1.2 Research Methodology	5
1.3 Organization of the Report.....	8
Chapter 2 Literature Review.....	9
2.1 BMD Approaches	9
2.1.1 Volumetric Design with Performance Verification	10
2.1.2 Performance-Modified Volumetric Design.....	11
2.1.3 Performance Design	11
2.2 Performance tests	11
2.2.1 Fracture Performance Tests.....	12
2.2.2 Rutting.....	14
2.3 Performance Tests for BMD.....	16
Chapter 3 Fracture Test Method for Nebraska BMD	21
3.1 Introduction.....	21
3.2 SCB Sample Preparation.....	21
3.3 SCB Test Set up and Data Analysis.....	22
3.4 Testing Variables	25
3.4.1 Methodology	25
3.4.2 Materials.....	25
3.4.3 Results and Discussion.....	26
3.5 Testing Fixtures	39
3.5.1 Materials.....	40

	3.5.2 Methodology	41
	3.5.3 Configurations of Test Fixtures.....	41
	3.5.4 Pairwise Comparison of Fixtures	43
	3.5.5 Assigning Specimen to Fixtures.....	44
	3.5.6 Results and Discussion.....	45
3.6	Summary	53
Chapter 4	Rutting Performance Test Method.....	54
4.1	Introduction.....	54
4.2	G-Stability (Gyratory Stability) Test Development.....	55
	4.2.1 G-Stability Test Set-up.....	55
	4.2.2 Sample fabrication.....	56
	4.2.3 Methodology	57
	4.2.4 Materials.....	57
	4.2.5 Results and Discussions	59
4.3	Correlation of G-Stability to Flow Number Test.....	65
4.4	Summary	67
Chapter 5	Performance Space Diagram (PSD) of Nebraska Mixtures.....	69
5.1	Performance Space Diagram.....	69
5.2	Short-term Performance Criteria.....	70
5.3	Long-term Performance Criteria.....	73
Chapter 6	Summary and Conclusions	74
References	76

List of Figures

Figure 1. Typical BMD Approaches: Three Options.....	3
Figure 2. The research methodology used in this study.....	7
Figure 3. Schematic illustration of three BMD approaches (NCHRP 20-07(406)).....	10
Figure 4. Fracture tests for AC mixtures: (a) DCT[27], (b) SENB[11], (c) SCB[24, 28, 29] , (d) IDEAL-CT[30] and (e) OT[31].	14
Figure 5. Rutting test for AC mixtures : (a) IDEAL-RT [33], (b) Hamburg [17, 31, 34], (c) Flow Number [15, 35] and (d) Dynamic Modulus [36].....	15
Figure 6. PSD from HWTT and DCT tests showing performance criteria for different mixtures [42].	18
Figure 7. Mixture collection: (a) from a mixture delivery truck and (b) containers of mixtures. 21	
Figure 8. SCB sample preparation: (a) compaction by SGC , (b) slicing, (c) halving and (d) notching.....	22
Figure 9. SCB fracture test: (a) test set-up and (b) fracture after SCB testing.	23
Figure 10. SCB test results and analysis.	24
Figure 11 Test results for the sample used to determine minimum number of replicates	26
Figure 12. Normality check of the sample.....	27
Figure 13. The minimum number of replicates versus the desired margin of error: (a) based on fracture energy, G_f , and (b) based on the flexibility index, FI	28
Figure 14. SCB test results at different thicknesses.....	28
Figure 15. Effect of specimen thickness on test results and their repeatability: (a) fracture energy and (b) flexibility index.....	30
Figure 16. SCB test results at varying notch lengths.	31
Figure 17. Effect of notch length on test results and their repeatability: (a) fracture energy and (b) flexibility index.	32
Figure 18. Off-center crack initiation for notch-less SCB specimens.	33
Figure 19. SCB test results at different loading rates.	34
Figure 20. Effect of loading rate on test results and their repeatability: (a) fracture energy and (b) flexibility index.	35
Figure 21. SCB test results at different temperatures.	37

Figure 22. Effect of testing temperature on test results and their repeatability: (a) fracture energy and (b) flexibility index.....	38
Figure 23. The nomenclature used on SCB test fixtures.	42
Figure 24. Configurations of investigated SCB load-support fixtures.	43
Figure 25. Scheme to reduce location-specific variability of SCB testing specimens.	45
Figure 26. SCB test results (load vs. LPD) of each fixture cases from eight replicates.	46
Figure 27. Average per fixture of SCB test results (load vs. LPD).	47
Figure 28. Effect of testing fixtures of fracture energy results and repeatability.	48
Figure 29. Effect of testing fixtures on flexibility index results and repeatability.	49
Figure 30. Effect of testing fixtures on maximum load results and repeatability.....	50
Figure 31. Effect of testing fixtures on cracking resistance index results and repeatability.	50
Figure 32. Effect of testing fixtures on slope properties: (a) pre-peak slope, (b) post-peak slope and (c) slope ratios	52
Figure 33. Flow number test: (a) set-up and (b) data analysis.....	55
Figure 34. Gyrotory stability test: (a) set-up and (b) results and data analysis.....	56
Figure 35. SCB sample preparation: (a) compaction by SGC and (b) slicing.....	56
Figure 36. Research methodology for G-Stability showing phases of development and correlation with FN.	57
Figure 37. Aggregate gradation of mixtures used in G-Stability development.	59
Figure 38. G-Stability testing results at different specimen thickness and mixture.	61
Figure 39. Determination of number of replicates: (a) sample fabrication and (b) environmental conditioning prior testing.	62
Figure 40. G-Stability test results for minimum replicates determination.....	62
Figure 41. Relationship between the margin of error and the minimum number of G-Stability replicates.	63
Figure 42. The sensitivity of the G-Stability Testing Method.....	64
Figure 43. Correlation between G-Stability vs. FN test results: (a) with the outlier and (b) without the outlier	66
Figure 44. G-Stability predicted from FN vs. experimental results.....	67
Figure 45. Performance space diagram of typical Nebraska mixtures in Nsengiyumva, Kim [74]..	69

Figure 46. Effect of quality of RAP on PSD of mixtures: high-quality RAP (15) and lower-quality RAP (23). 70

Figure 47. PSD of high-RAP mixtures with performance criteria..... 72

Figure 48. PSD of all mixtures tested here showing the criteria in Table 6 and FI of 6..... 73

List of Tables

Table 1. The state of practice of balanced mixture design (summarized from West, Rodezno [46], NCHRP 20-07/Task 406).....	20
Table 2. Comparison process to extract the effect of fixtures components	44
Table 3. Recommended values for SCB testing variables	53
Table 4. Key Characteristics of Mixtures Used in Here	58
Table 5. Testing Results Used in Correlation of G-Stability to Flow Number.....	65
Table 6 Performance Criteria for Rutting in FN and G-Stability	71

Acknowledgment

The authors thank the Nebraska Department of Transportation (NDOT) for the financial support needed to complete this study. In particular, the authors thank NDOT Technical Advisory Committee (TAC) for their technical support and invaluable discussions/comments.

Disclaimer

The contents of this report reflect the views of the authors, who are responsible for the facts and the accuracy of the information presented herein. The contents do not necessarily reflect the official views or policies neither of the Nebraska Department of Transportations nor the University of Nebraska-Lincoln. This report does not constitute a standard, specification, or regulation. Trade or manufacturers' names, which may appear in this report, are cited only because they are considered essential to the objectives of the report.

The United States (U.S.) government and the State of Nebraska do not endorse products or manufacturers. This material is based upon work supported by the Federal Highway Administration under SPR-1(18) M070. Any opinions, findings and conclusions or recommendations expressed in this publication are those of the author(s) and do not necessarily reflect the views of the Federal Highway Administration.”

Abstract

Balanced mixture design is an alternative asphalt concrete design method that incorporates the performance of mixtures during the design. Balanced mixture design consists of performance test methods and performance criteria. Compared to the existing Superpave design method which mostly relies on volumetrics to design mixtures, balanced mixture design is more suited to account for performance improvements originating from reclaimed asphalt pavement and other foreign additives such as rejuvenators, warm-mix asphalt additives, polymers, and anti-stripping agents. This study investigated the feasibility of the implementation of balanced mixture design in Nebraska mixtures by exploring appropriate test methods (i.e., for fracture and rutting) and method of selection of performance criteria. For the fracture test, the semicircular bend test method was selected and investigated for the appropriate testing conditions that can provide repeatable results. These testing conditions included: the number of replicates, specimen thickness, testing temperature, notch length, and loading rate. Also, the effect of the semicircular bend testing configurations on the test results and their repeatability was explored. For the rutting performance test, a simple rutting test called Gyrotory stability was explored by determining critical testing conditions that can aid repeatable results and practical implementation. The validity of the newly developed Gyrotory stability test was accomplished by correlating its test results to that of the established flow number test. The correlation showed interchangeability between the Gyrotory stability and the flow number, which demonstrated the feasibility of the Gyrotory stability as a rutting performance test. Finally, the two performance tests (semicircular bending and Gyrotory stability) were conducted for typical Nebraska asphalt concrete mixtures and several additional mixtures including high amounts of recycled materials with rejuvenating agents. Test results were incorporated with a performance space diagram.

Chapter 1 Introduction

Asphalt Concrete (AC) mixture was born out of the desire to fulfill the growing need for long-lasting pavement and as a means to dispose of bitumen, which is the byproduct of petroleum distillation. The bitumen henceforth referred to as asphalt, served as a binder of loose aggregates to increase their cohesiveness and increase service life. Besides, the binder provided benefits such as smoothing of the roadway and moisture damage protection. Naturally, the main challenge of the newly invented construction materials was to determine the optimum design of component proportion that would provide the desired service lifespan. Furthermore, the economic aspect of the AC mixture design was also of interest cost savings related to raw materials acquisition. As a result, early efforts were undertaken to attempt to solve the mixture design-related challenges.

The first widely adopted AC design method was the Marshall method which was developed by Bruce Marshall for the Mississippi Highway Department in the late 30's. The key component of the method was to determine the asphalt content at which the stability of mixtures was maximized. This was achieved by preparing several mixtures at different increasing asphalt contents. Subsequently, cylindrical specimens of four inches in diameter and 2 ½ inches in height were prepared and tested for stability. The Marshall method had several shortcomings related to laboratory sample compaction, binder, and aggregate selections. The compaction of samples for the Marshall testing used a drop hammer and resulted in broken flat aggregates, which was in contrast with field compaction that used roller compactors. Furthermore, the Marshall method did not consider climate- and region-specific mixture design which resulted in a significantly different performance of mixtures depending on climates. Finally, the Marshall design method placed less emphasis on aggregate gradation design and resulted in premature rutting and raveling of pavement.

The Superpave design method was developed by the SHRP (Strategic Highway Research Program) to address the limitations of the Marshall method. Specifically, Superpave allowed for traffic-based materials design and selection and introduced load advanced asphalt binder selection to suit different climates. In addition, Superpave developed a new mixture analysis and testing method which included the SGC (Superpave gyratory compactor) for sample fabrication. The Superpave focused on mixture design in terms of volumetric proportions occupied by each of the components in AC mixtures. Several volumetric related indicators such as VMA (voids in mineral aggregates), VFA (voids filled with asphalt) were introduced in addition to traditional indicators

such as air voids (V_{air}), and asphalt contents. Furthermore, the Superpave design method introduced a new PG (performance grade) system for asphalt binder performance which specified lower and upper-temperature limits of binders.

The limitation of the Superpave design method emerged from its heavy reliance on mixture volumetric characteristics (i.e., VMA, VFA, V_{air}) and thus unable to account for the effects of RAP (recycled asphalt pavement) and additives. As a result, researchers have proposed a performance-oriented AC mixture design by mainly focusing on the balance between rutting and fracture resistances of mixtures rather than volumetrics. The resulting design method is called balanced mixture design (BMD), which pursues a balance between cracking and rutting performances of mixtures. The two properties (i.e., rutting and fracture) often require opposing characteristics from mixtures such that soft mixtures resist better cracking while stiff mixtures resist better permanent deformation (i.e., rutting) [1]. Hence, BMD mixture design involves balancing the two core properties from which a balance can be reached by varying the composition of mixtures [2] with minimal or without consideration to mixture volumetrics.

The BMD concept has been getting increased attention from the pavement community. The common form on BMD incorporates two or more mechanical performance tests, such as a rutting test and a cracking test to characterize mixture resistance to common forms of distresses (i.e., fracture and rutting). The BMD solves the issue in the current Superpave volumetric mix design where the proportioning of the aggregates and the asphalt binder relies primarily on empirical aggregate quality characteristics and mixture volumetric properties. However, the calculation of the volumetric properties is highly dependent on an accurate determination of the specific gravity, which is extremely sensitive to minute changes in the mixture. The complexity and inaccuracy of Superpave volumetric mixture design further increase with the incorporation of reclaimed asphalt pavements (RAP) [3-6] and foreign additives such as antistripping and rejuvenating agents [3], antioxidants [7], polymers [8], and fibers [9].

Since components of an AC mixture minimally affect its volumetrics, the contribution of RAP and other additives can be overlooked when using the Superpave method. Therefore, performance tests need to be included as part of the AC mixture design procedure to help ensure desirable pavement performance in the field. To include any mixture performance test in the BMD procedure, criteria for the test result must be established based on a strong relationship to field performance and specific mixtures used in the state.

In September 2015, the Federal Highway Administration (FHWA) Expert Task Group on Mixtures and Construction formed a BMD Task Force, which defined BMD as “asphalt mix design using performance tests on appropriately conditioned specimens that address multiple modes of distress taking into consideration mix aging, traffic, climate, and location within the pavement structure.” The Task Force also identified three potential approaches to the use of BMD depending on how much importance is given to volumetrics: (1) volumetric design with performance verification, (2) performance-modified volumetric mix design, and (3) performance design (Figure 1).

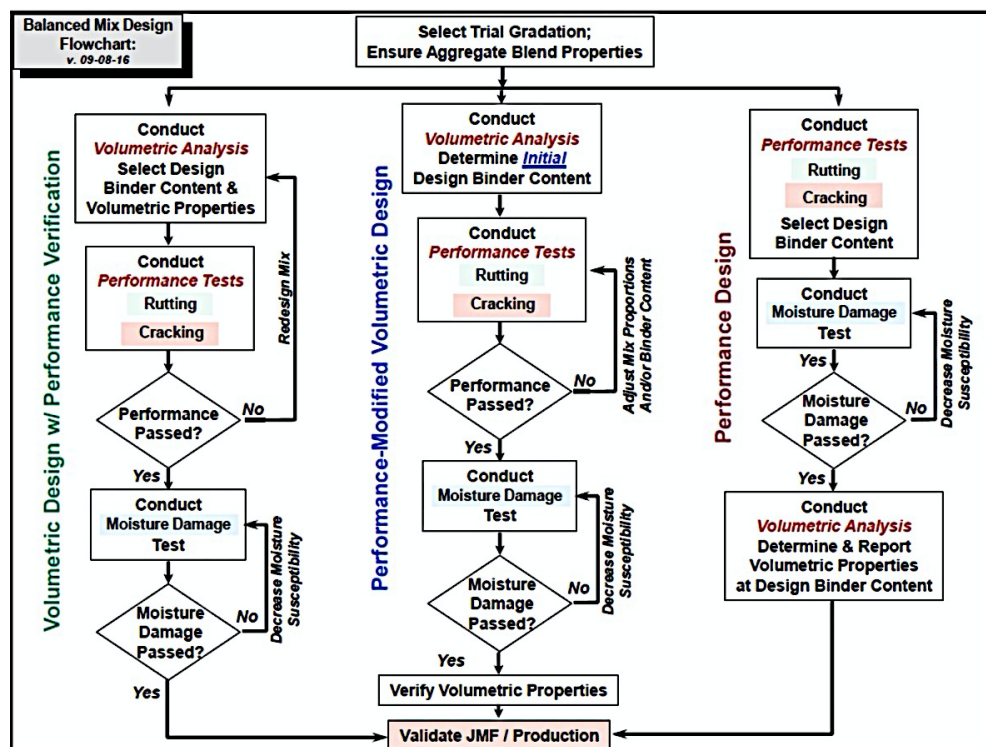


Figure 1. Typical BMD Approaches: Three Options

The first approach is volumetric design with performance verification (VDPV) in which mixtures must satisfy the performance criteria after mixture design using Superpave (i.e., volumetrics). If the mixture does not pass performance tests, the entire mix design process is repeated. This approach is currently used in Illinois, Louisiana, New Jersey, Texas, and Wisconsin.

The second approach is the performance modified volumetric design (PMVD) in which volumetric designed mixtures ultimately need only to satisfy performance criteria. This approach

begins with the Superpave mix design method to establish an initial aggregate blend and asphalt content. Adjustments in the mix proportions are then permitted to meet the performance tests. The final design may not be required to meet all the traditional Superpave criteria. California currently uses this approach.

Finally, the performance design (PD) in which volumetrics of mixtures are excluded during design. However, when design using PD, volumetrics to be considered as a recommendation rather than a requirement. Specifically, this approach skips the volumetric mix design and starts with an evaluation of mix trials (possibly multiple gradation trial blends and asphalt contents) using the performance tests. Minimum requirements may be set for asphalt binder and aggregate properties. Traditional volumetric criteria may be used as non-mandatory guides but not as design criteria. This approach is not currently used but could be a viable option.

The commonality of the three approaches of BMD is through the key components: test methods and performance criteria. The test methods are chosen to evaluate the resistance of mixtures to common AC pavement distresses such as a fracture (i.e., cracking) and rutting. Next, performance criteria are used to establish acceptable ranges of test results, which are indicative of cracking and rutting performances.

Over the past few decades, numerous performance tests have been developed by different researchers to evaluate the rutting resistance, cracking resistance, and moisture susceptibility of asphalt mixtures. Considering the different mechanisms of crack initiation and propagation, mixture cracking tests can be further categorized into thermal cracking, reflection cracking, bottom-up fatigue cracking, and top-down fatigue cracking. To include any mixture performance test in the BMD procedure, criteria for the test result should be established based on a strong relationship to field performance.

To evaluate fracture performance of mixtures, several tests have been proposed such as DCT [10], SNEB [11], SCB [12], IDEAL-CT [13]. Among them, the SCB has been attractive to characterize fracture performance of AC mixtures [12, 14, 15], due to simplicity, higher repeatability, and practicality. Also, the SCB test method has demonstrated the ability to detect an existing difference in AC mixtures [12, 14, 15]. Given that the key factors involved in selecting test methods are the test repeatability/variability, equipment availability and cost, and sensitivity to different mixtures, the SCB test becomes well suited to performance test mixtures for BMD application.

The rutting test of AC mixtures aims at simulating permanent deformation on AC specimens until a predetermined failure criterion has been reached. The test results are then analyzed to extract a rutting-related indicator. Over the past decades, several rutting tests have been proposed such as the APA (asphalt pavement analyzer) [16], HWTT (Hamburg Wheel Track Tester) [17], and IDEAL-RT [37], and FN (flow number) [18]. FN is considered to be the least empirical test method. FN is also known as the simple performance test. It was proposed by Witczak, Pellinen [19] and involves pulse loading and unloading of a specimen and recording the accumulated strains over time. Similar to SCB test results for fracture, FN rutting results have demonstrated sensitivity to mixtures rutting resistance [18] and with field rutting performance [20, 21].

However, unlike SCB, FN involves a multitude of testing-related complexities that reduces practicality and simplicity. For example, FN requires complex equipment capable of cyclic loading and a robust data acquisition system. In addition, identifying testing parameters such as temperature, loading stress and contact stress is cumbersome and time-consuming. Finally, data analysis of FN test results requires differentiating accumulated strains curve with respect to loading cycles (by first fitting a function to the curve) which further discourages the test to be readily and widely implemented for BMD purposes. Hence, despite the advantages of FN, the associated complexities make it difficult to incorporate into BMD. This exposes a need for a practical, simpler, and sensitive rutting test capable of detecting differences in mixtures and presents a strong correlation with existing sophisticated tests towards the wider implementation of BMD.

1.1 Research Objective

The overall goal of this study is to examine the feasibility of the BMD approach for Nebraska mixtures and to develop a potential implementation plan of the method.

1.2 Research Methodology

To meet the objective, a methodology was proposed which involved the development of fracture and rutting performance test methods and application of the developed tests into BMD of Nebraska mixtures. The SCB geometry was selected for the fracture performance test and was developed by first considering the effects of critical testing variables on the repeatability of test results followed by investigating the effects of testing configurations on SCB test results. SCB testing variables

investigated were the minimum recommended number of specimens (n), specimen thickness (t), notch length (nl), loading rate (lr), and the testing temperature (T). For the SCB fixtures, the effects of components such as the mid-span jig, rolling-freedom, and the shape of rolling surfaces were investigated for their effects on test results and their repeatability.

For the rutting test method, a study was conducted to investigate whether a simple test could be performed at the time of mixture design that would have a strong correlation with more sophisticated performance (i.e., FN) testing. The simple test was selected to use a disc-shaped specimen and was named Gyrotory Stability (G-Stability) after the SGC (Superpave gyrotory compactor) that is used to prepare the specimen. Several critical testing parameters of the G-Stability method were temperature, loading rate, specimen thickness, and the number of replicates. They were examined based on testing repeatability and practicality. The G-Stability test results were compared to a counterpart rutting performance test: FN (flow number) to ensure compatibility of the practical G-Stability test with a more sophisticated performance test. Test results were then used in a PSD (performance space diagram), which can lead to the identification of preliminary performance criteria of Nebraska mixtures. The research method adopted in this study is shown in Figure 1.

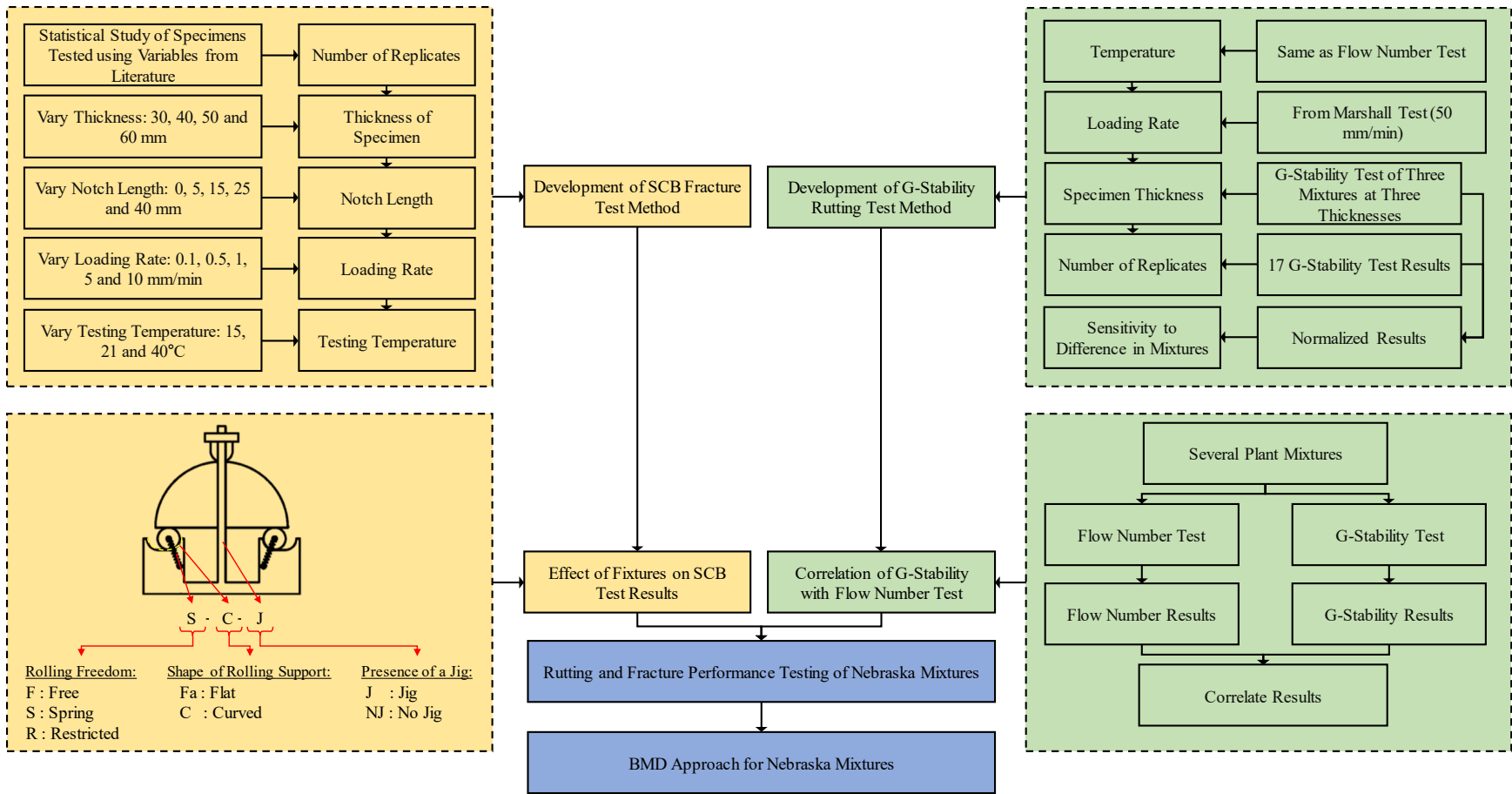


Figure 1. The research methodology used in this study.

1.3 Organization of the Report

This report consists of six chapters. This chapter (introduction) presents the motivation of this research project, the current knowledge gap, and the resulting objective of this study. Subsequently, Chapter 2 (literature review) presents a summary of the relevant studies. Chapter 3 shows efforts to develop the SCB fracture test to be used in the Nebraska BMD. Chapter 4 shows efforts to develop a rutting performance test for Nebraska BMD. As mentioned, the G-Stability test was explored by comparing the results with FN test results. Chapter 5 includes the process of using test results (i.e., SCB and G-Stability of Nebraska AC mixtures) to develop the PSD and resulting performance criteria. Finally, Chapter 6 summarizes findings and conclusions from this project.

Chapter 2 Literature Review

The design of AC mixtures involves several aspects that influence the performance of the resulting mixtures such as aggregates, asphalt content, and air content. In the traditional sense, the AC mixture design considered proportions of the mentioned factors of mixtures. However, in the bid of improving service life and durability, there has been an increase in the additives to AC whose contributions cannot be accurately assessed by the volumetrics-based approach to design AC. Additives such as polymers, warm-mix additives, antistripping may significantly impact the performance of AC mixtures while minimally affecting the volumetrics.

Per Federal Highway Administration (FHWA) Expert Task Group (ETG) on Mixtures and Construction, BMD is defined as “asphalt mixture design using performance tests on appropriately conditioned specimens that address multiple modes of distress taking into consideration mix aging, traffic, climate and location within the pavement structure.” Also, BMD is classified as an index-based performance engineered mixture design (PEMD) as opposed to predictive PEMD which requires mechanical-empirical (ME) simulation [22]. It should be noted that BMD/PEMD is a component of the broader vision by the Federal Highway Administration (FHWA) of performance-engineered pavement (PEP). Beyond PEMD, FHWA envisions optimization to pavement structural and mixture design to address common distress in the Nation’s highway infrastructure while providing a room for innovation.

BMD process requires performance testing of AC mixtures for common distresses such as rutting and cracking which must meet an established criterion. As a result, the key components of BMD are performance tests and performance criteria. BMD originated in Texas A&M Transportation Institute by Zhou, Hu [2] where the authors used Hamburg Wheel Tracking Test (HWTT) and Overlay Tester (OT) test methods to evaluate and balance rutting and cracking resistance AC mixtures, respectively. Studies that have then been conducted proposed implementing BMD with different and performance tests and criteria.

2.1 BMD Approaches

As mentioned in the introduction chapter, there are different approaches to which BMD can be implemented depending on how much importance is carried by volumetric. Despite the differences, all BMD approaches need to satisfy performance and moisture susceptibility criteria. Figure 2 by

NCHRP 20-07(406) graphically shows flowcharts of three different BMD approaches that can be used for AC mixtures.

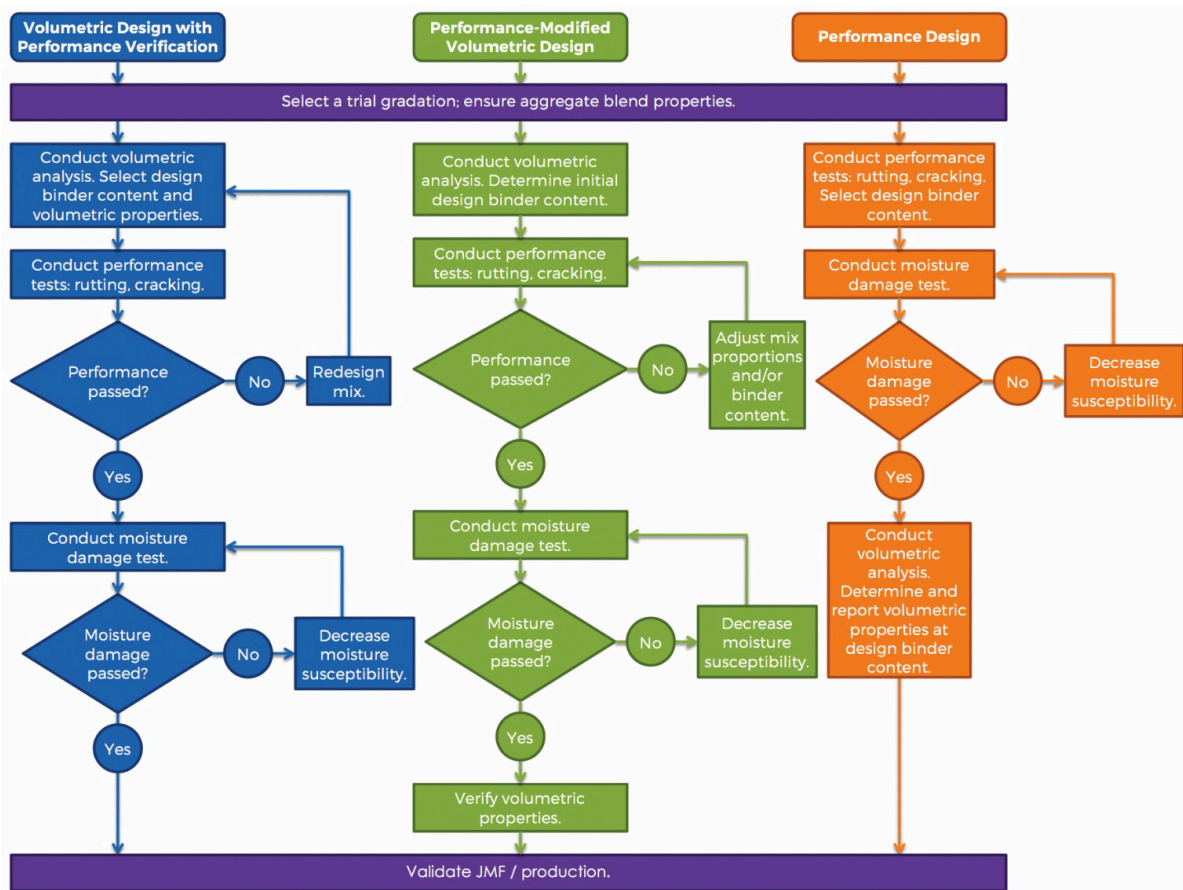


Figure 2. Schematic illustration of three BMD approaches (NCHRP 20-07(406))

2.1.1 Volumetric Design with Performance Verification

The volumetric design with performance verification (VDPV) is the application of BMD in which both the volumetrics and performance criteria need to be satisfied before the design is considered complete. A mixture that fails the performance part can be improved by adjusting the source or gradation of aggregates or by changing the source or composition of the asphalt binder. VDPV is popular among state DoTs since it supplements the exiting volumetrics-based methods. However, once a mixture fails the performance test, then the whole mixtures have to be redesigned following Superpave (i.e., AASHTO R 35). Even so, the redesigned mixture is not guaranteed to meet the

performance criteria while still satisfying Superpave design. As a result, VDPV can sometimes be cumbersome to implement by mixture designers given the constraints.

2.1.2 Performance-Modified Volumetric Design

To address the elaborated constraints issue of VDPV, performance-modified volumetric design (PMVD) was introduced. In this method, the AC mixture is first designed to meet volumetric criteria per Superpave method followed by performance criteria checking. Subsequently, if the mixture fails the performance criteria, any of asphalt content, asphalt source, aggregate gradation, or aggregate source can be adjusted to meet the performance criteria without regard to the volumetric requirements. Therefore, PMVD is more flexible and offers a more performance-oriented and practice-friendly version than VDPV. As a result, PMVD only relies on volumetrics as a basis to determine the initial asphalt-aggregate combination and then modify the mix to meet performance criteria. The most common to improve/modify mixture performance with PMVD is to vary the optimum binder content by $\pm 0.5\%$ and then check for performance. Higher asphalt content typically improves fracture resistance while the lower end improves rutting resistance.

2.1.3 Performance Design

The final form of BMD is the performance design (PD) method in which there is absence or limited consideration of the volumetric requirements at any stage of mixture design. As a result, PD relies solely on performance testing to establish proportions of mixture components. To simplify the PD method, traditional volumetric properties such as V_{air} , VMA, minimum asphalt content, and aggregate gradation are used as recommendations rather than requirements. Before the mixture can be approved as a JMF (job-mix formula) a moisture sensitivity test is performed to ensure the durability of the mix. However, once a mixture design that meets performance and moisture damage criteria has been found, its volumetrics are recorded and used in subsequent projects. From there, if the design mixture needs to be adapted for a new project with a different performance requirement then the mixture serves as the starting point.

2.2 Performance tests

Performance tests are among the key components of BMD methods. They allow designers to assess the performance of a mixture in the laboratory before being approved for deployment. The tests

are selected to evaluate mixtures resistance to common distresses which are cracking and rutting. To select a test, different factors such as: accessibility, availability of the test standard, simplicity of the test, accuracy, repeatability, and variability. Towards these, several researchers have proposed cracking and rutting performance test.

2.2.1 *Fracture Performance Tests*

2.2.1.1 SCB (Semi-Circular Bending)

The semi-circular bending test (Figure 4c) was initially developed by Chong and Kuruppu [23] aiming to simplify fracture testing in rock materials. Since the test has been widely adopted in the asphalt community due to its simplicity, repeatability, and practicality. The test involves and semi-circular specimen with a fracture notch in the bottom (i.e., flat side). The specimen is then loaded from the top (i.e., curved side) at a given loading rate until failure. The results are then interpreted by calculating a fracture-related indicator such as fracture energy, cracking resistance index, and flexibility index [24, 25].

2.2.1.2 DCT (Disk-Shaped Compact Tension Test)

DCT (Figure 4a) was adopted from ASTM E399 (standard test method for linear-elastic plane-strain fracture toughness K_{Ic} of metallic materials) to be used on the AC mixture by Wagoner, Buttlar [10]. Wagoner, Buttlar [10]. The specimens for DCT are disk-shaped with an offset cut from one end on which a notch perpendicular to the cut is inserted. In addition, two holes loading holes located at each side of the notch are drilled and used to load the specimen during testing. DCT specimens have the advantage of having a considerably larger fracture ligament compared to other fracture test methods which can help improve the repeatability of results. However, sample preparation for DCT is delicate and requires significant experience to properly achieve. For example, failure can happen at the loading holes in heterogeneous materials such as AC mixtures [10]. As result, to minimize the sample preparation and testing issues while ensuring repeatability, ASTM D7313 (standard test method for determining fracture energy of asphalt-aggregate mixtures using the disk-shaped compact tension geometry) was developed for AC mixtures.

2.2.1.3 OT (Overlay Tester)

The overlay tester was developed by Zhou and Scullion [26] as a method to evaluate the cracking resistance of AC mixtures overlays. The test simulates an existing cracking crack in the bottom layer of the overlays which then expands. The overlay tester was developed by Zhou and Scullion [26] as a method to evaluate the cracking resistance of AC mixtures overlays. The test simulates an existing crack in the bottom layer of the overlays which then expands (Figure 4e). This test involves an unconventional specimen which is a hybrid disk and beams. The specimen is then glued on the bottom support plates which are subsequently loaded cyclically at room temperature for 24 hours [17]. Although this test can more realistically replicate overlay loading of AC mixtures, the specimen preparation (i.e., cutting and gluing) and the long testing time reduces the practicality of the test. Also, there is a probability debonding between the specimen and the bottom support fixture which can lead to failure of the test.

2.2.1.4 IDEAL-CT (Indirect Tensile Asphalt Cracking Test)

The indirect tensile asphalt cracking test was developed by Zhou, Im [13] in bid to simplify fracture testing AC (Figure 4d). The test was meant as a practical and easy method to quickly evaluate the fracture resistance of mixtures, especially during QA/QC. Specimens of 62 mm thickness are loaded with an LPD (load-point displacement) rate of 50 mm/min to induce indirect tensile loads at room temperature. Test results are then analyzed to infer fracture-related indicators (e.g., fracture energy). Although this test is simple and practical, there is a possibility of significant stress localization round LPD which can dilute the observed results. In addition, the lack of a notch in the specimen complicates the application of the theory of fracture mechanics which limits the interpretation of the results beyond QA/QC-related purposes.

2.2.1.5 Single Edge Notched Beam (SNEB)

The single edge notched beam was developed by Wagoner, Buttlar [11] and used beam-shaped specimens which have a notch in the middle (Figure 4b). Testing is conducted in the CMOD controlled mode and the testing temperature is typically low (e.g., -10C). This test has the advantage of having numerical and analytical solutions using classical fracture mechanics. However, SNEB is disadvantaged by complicated sample preparation and testing set-up which

reduces the practicality of the test in AC where compacted samples and cores are typically cylindrical.

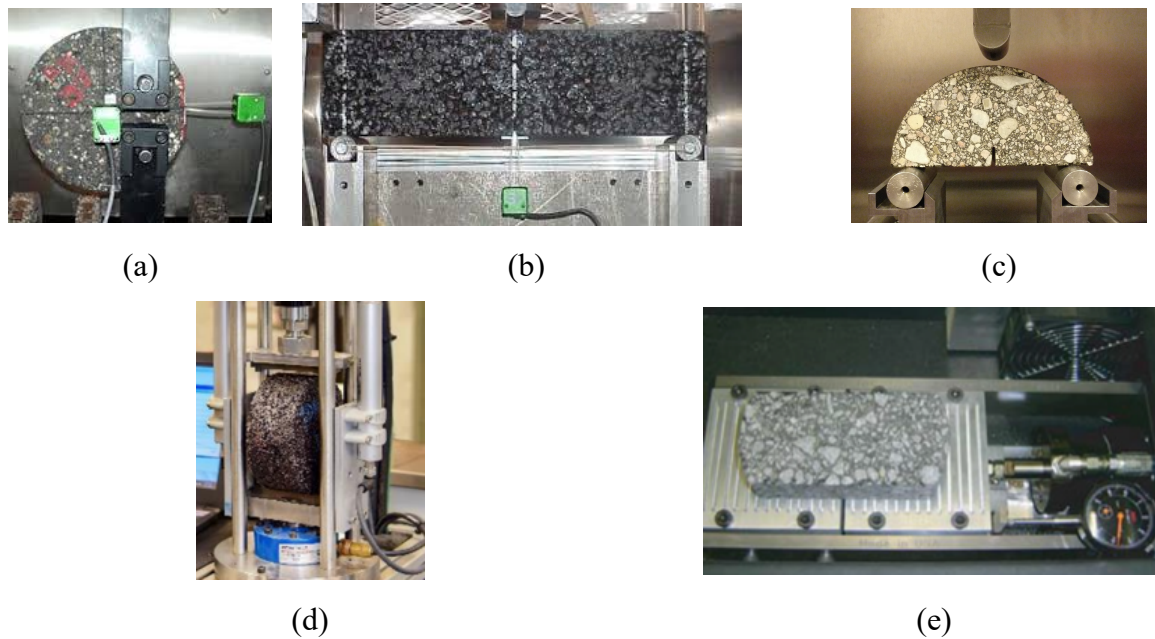


Figure 4. Fracture tests for AC mixtures: (a) DCT[27], (b) SENB[11], (c) SCB[24, 28, 29] , (d) IDEAL-CT[30] and (e) OT[31].

2.2.2 Rutting

2.2.2.1 FN (Flow Number)

Flow number test was recommended by the NCHRP Project 9-19 as part of the SPT (simple performance test) program. FN consists of cyclically loading cylindrical AC specimens for 0.1 seconds with a rest period of 0.9 seconds. The test continues until the flow is achieved or until 10,000 loading cycles are reached. Testing temperature and deviatoric stress for FN are selected to achieve flow within the 10,000 cycles or 2.778 hours. FN has the advantage of being a fundamental test which simulates pavement loading condition where a truck passes followed by a short rest period at high temperature. FN has shown a good correlation with field performance of the AC mixture [32]. The main disadvantage of FN is the complexity of the test which requires a robust enough equipment that can accurately apply cyclic loading and maintain the temperature.

In addition, data analysis of FN involves finding a derivative of the test results which require curve fitting. This further inhibits the simplicity, application, and practicality of FN despite its accuracy.

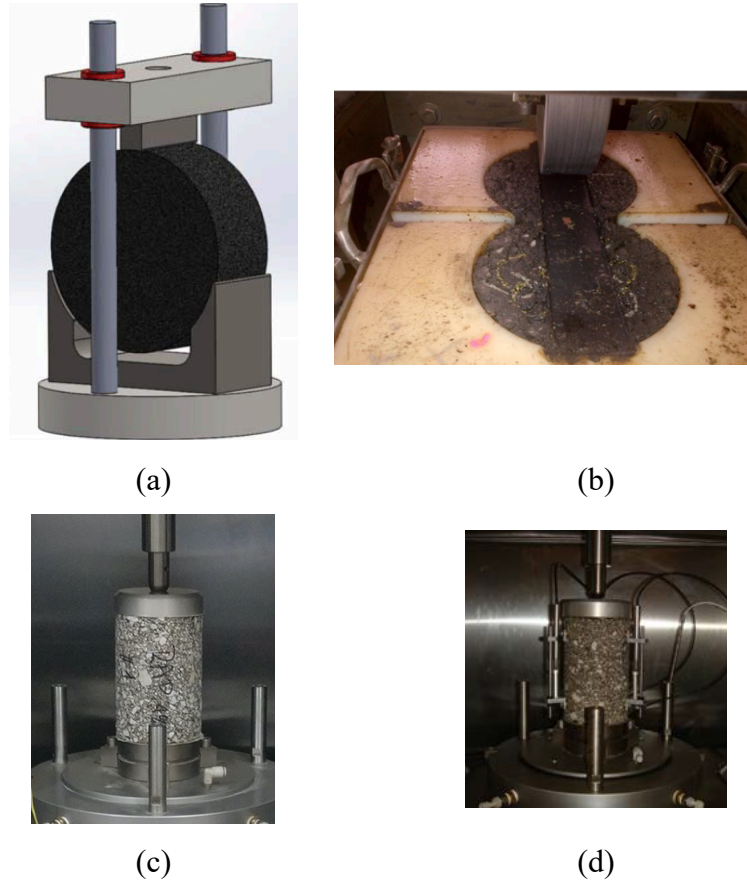


Figure 3. Rutting test for AC mixtures : (a) IDEAL-RT [33], (b) Hamburg [17, 31, 34], (c) Flow Number [15, 35] and (d) Dynamic Modulus [36]

2.2.2.2 IDEAL-RT (Indirect Tensile Asphalt Rutting Test)

The indirect tensile asphalt rutting test was recently proposed by Fujie Zhou and Sun [33] in a bid to simplify rutting test during mixture design and QA/QC phases. The IDEAL-RT is essentially IDEAL-CT with exception of increased testing temperature and a different bottom fixture. In the rutting test, a Marshall bottom fixture is used to induce shear failure in the specimen and the temperature is raised to 50°C and the loading rate is 50 mm/min. IDEAL-RT has correlated well with field performance observation of mixtures and showed good repeatability. The main disadvantage of this test is that it relies on shear deformation to predict rutting which is typically

a top-down phenomenon. In addition, test specimens are loaded from the top using a small contact area which does not reflect field conditions where rutting distress is caused by large tires from heavy trucks.

2.2.2.3 HWTT (Hamburg Wheel Track Tester)

The Hamburg wheel track tester was developed in Germany by Aschenbrener [34] to evaluate the rutting of asphaltic mixtures. The test is considered a torture test in which specimens (typically two disks from SGC) are loaded using a steel wheel until failure rutting depth. Moisture effect on the rutting performance of the mixture can also be evaluated using the HWTT by simply introducing water to the test chamber during testing. The test was conducted according to AASHTO T324: Standard Method of Test for Hamburg Wheel-Track Testing of Compacted Hot Mix Asphalt (HMA). The specimens are kept at the testing temperature of 40°C while the wheel passes 52 times loaded at 705 N [17]. Although HWTT has been found to correlate well with field performance, the complexity of the test limits its practicality and repeatability.

2.3 Performance Tests for BMD

Several studies have explored using the performance test aforementioned to implement the balanced mixture design. Cooper III, Mohammad [37] used the SCB test to evaluate fracture potential of Louisiana mixtures towards BMD implementation. In the cited study, the J-integral (i.e., critical strain energy release rate) was used as a fracture indicator. Although J-integral has the advantage of being based on principles of fracture mechanics, it required test results at multiple notch lengths (e.g., 25.4 mm, 31.8 mm, and 38 mm notch lengths) which may discourage its adoption for practical purposes. In the cited study, the performance criterion was selected to be fracture energy of 0.5 kJ/m² based on overall the average of test results from several Louisiana mixtures [38]. Interestingly, the same performance criteria for fracture was applied to all mixtures despite that mixtures with modified binders having higher fracture resistance. In contrast, for rutting resistance efforts conducted in the same study [37], the criteria were specific to binder types used mixtures (e.g., modified or unmodified).

Bahia, Teymourpour [39] conducted a study to examine the feasibility of BMD implementation for Wisconsin DOT (WisDOT). Two versions of SCB were used to evaluate fatigue (i.e., intermediate temperature) and thermal (i.e., low temperature) cracking of AC

mixtures. For fatigue cracking the I-FIT (Illinois Flexibility Index Test) was adopted, while the SCB test developed by Li and Marasteanu [40] was adopted for thermal cracking. It is noteworthy that both versions of SCB test methods utilized a single notch thus eliminating the multiple notches required by Cooper III, Mohammad [37]. The differences between the two SCB tests used in the study were the loading rate: 50 mm/min for I-FIT vs. 0.5 mm/min for SCB by Li and Marasteanu [40] and the fracture-related indicator used: Flexibility Index (FI) for I-FIT vs. fracture energy (G_f) for SCB by Li and Marasteanu [40]. After conducting SCB tests of several mixtures with different volumetrics and composition, Bahia, Teymourpour [39], concluded that FI provided results with a wide range in which mixtures could be distinguished. In contrast, the range of G_f resulted in a relatively narrower range of values compared to that of FI tested on the same mixtures. As a result, FI was recommended to be included in the WisDOT BMD for intermediate performance test. For the low-temperature, G_f was recommended SCB test results due to difficulty in calculating the post-peak slope required to obtain FI.

Kim, Mohammad [41] conducted a study about performance-based mixture design in the State of Louisiana using loaded wheel tracking (LWT) test and SCB test to measure rutting and fracture performances, respectively. The study compared fracture results as J_c in kJ/m² and rut depth from LWT in mm to actual field performance which led to the determination of performance criteria. For fracture, a criterion of 0.5 and 0.6 kJ/m² of J_c was established for low and high traffic, respectively. For the rutting criteria, LWT rut depths of 10 and 6 mm were selected for low and high traffic, respectively. The study then combined the test methods and the criteria to propose PBS (performance-based specifications) for Louisiana. It is noteworthy that the LWT test used in the cited study was the HWTT and conducted according to AASHTO T 324.

Buttlar, Hill [42] used HWTT and DCT test results to establish a PSD (performance space diagram) for Illinois AC mixtures (Figure 6). In the study, the HWTT rut depth was plotted on the y-axis in descending order from bottom to top while DCT fracture energy was plotted on the x-axis in ascending order. The resulting plot then designated regions classifying mixtures based on their rutting and cracking performance relative to their expected traffic levels. It is noted that while all mixtures satisfied the same rutting requirement, the cracking was traffic dependent as such, high traffic demands high fracture passing criteria. The study showed that using polymer modification of binder can help improve both fracture and rutting performances and that SAM (stone matrix asphalt) typically satisfied the high traffic criteria. Jahangiri, Majidifard [43] used

HWTT-DCT PSD to show that most RAP (reclaimed asphalt pavement) and RAS (reclaimed asphalt shingles) mixtures were relatively brittle compared to virgin mixtures and thus failed to pass fracture energy criteria (i.e., DCT). This highlights the need of improving RAP mixtures containing a significant percentage of RAP (e.g., > 40%) using options such as rejuvenators and WMA additives [44].

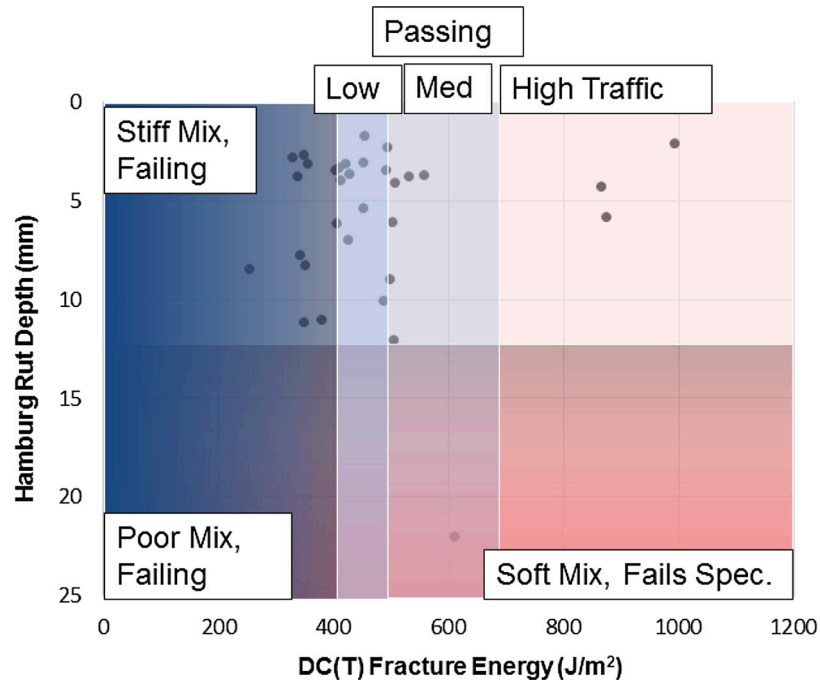


Figure 6. PSD from HWTT and DCT tests showing performance criteria for different mixtures [42].

Around the US, several states (e.g., Louisiana, New Mexico, Oklahoma, South Dakota, Wisconsin) have studied the feasibility of implementation of BMD to replace the Superpave volumetric design method. Other states (such as California, Florida, Georgia, Illinois, Texas, Utah, etc.) have adopted BMD to a certain extent in their mixture design which includes performance tests and criteria [45]. States located in cold climates (e.g., Minnesota) tend to focus on fracture/cracking while States in warmer climates (e.g., Georgia and Florida) emphasize meeting deformation criteria than cracking. The most common fracture tests adopted or being considered by the States for BMD include SCB, DCT, and OT, albeit with different standards and test conditions. For rutting, HWTT and APA both at high temperature (typically > 40°C) have been adopted or under consideration. Each state tends to choose its performance criteria by correlating

the test results and field performance. Most fracture tests are conducted at room temperature on two hours oven (at 135°C) aged mixtures. Finally, most States require mixtures to pass moisture susceptibility test per AASHTO T283: Resistance of compacted hot mix asphalt (HMA) to moisture-induced damage.

Table 1 summarizes the current state of practice of BMD implementation by different states West, Rodezno [46]. As can be seen, only four states (IL, NJ, OK, and TX) have fully implemented the BMD in their mixture design. The remaining states are currently conducting research and field performance monitoring to establish appropriate tests and criteria. The states without finalized BMD method have adopted preliminary performance testing and criteria that are summarized in Table 1. It should be noted that the different design traffic requires different performance criteria with higher traffic requiring a higher performance limit (e.g., higher fracture energy).

Table 1. The state of practice of balanced mixture design (summarized from West, Rodezno [46], NCHRP 20-07/Task 406).

State	Approach	Distress	Test	Criterion
California		Rutting Cracking	HWTT at 50C AASHTO T 321	< 12.5 mm at 20,000 passes
Florida		Rutting Cracking	APA at 64C —	< 4.5 mm at 8,000 cycles —
Georgia		Rutting Cracking	HWTT at 50C —	< 12.5 mm at 20,000 passes —
Illinois	1	Rutting Cracking	HWTT at 50C I-FIT (AASHTO TP 124)	< 12.5 mm at 20,000 passes > 8
Iowa		Rutting Cracking	HWTT at 50C DCT (under consideration)	< 8 mm at 8,000 passes
Louisiana		Rutting Cracking	HWTT at 50C SCB-Jc at 25C	< 10 mm at 20,000 passes > 0.6 kJ/m ²
Minnesota		Rutting Cracking	— DCT-Gf (ASTM D7313)	— > 690 J/m ²
New Jersey	1	Rutting Cracking	APA at 64C OT (NJDOT B-10) at 25C	< 7 mm at 8,000 cycles > 700 cycles
Ohio		Rutting Cracking	APA at 54.4C —	< 5 mm at 8,000 cycles —
Oklahoma	2	Rutting Cracking	HWTT at 50C I-FIT (AASHTO TP 124)	< 12.5 mm at 20,000 passes —
South Dakota		Rutting Cracking	APA at 64C —	< 8 mm at 8,000 cycles —
Texas	1	Rutting Cracking	HWTT (Tex-242-F) at 50C OT (Tex-248-F) at 25C	> 10,000 and > 20,000 passes at 12.5 mm rut depth > 150 and >300 cycles
Utah		Rutting Cracking	HWTT at 46C - 50C —	< 10 mm at 20,000 passes —
Wisconsin		Rutting Cracking* Cracking**	HWTT (AASHTO T 324) DCT-Gf (ASTM D7313) SCB-Jc (ASTM D8044) at 25C	> 5,000 and > 10,000 passes at 12.5 mm rut depth > 400 J/m ² > 0.4 kJ/m ²

* Low-temperature test, and ** Intermediate temperature test

Chapter 3 Fracture Test Method for Nebraska BMD

This chapter is composed of two parts dedicated to the development efforts for the SCB fracture test at intermediate service temperatures and investigation of the testing configuration of the SCB test method.

3.1 Introduction

As mentioned above, SCB has shown the benefits of being a simple and practical test that can be conducted both on laboratory and field cores. Also, the SCB test has shown the potential of improving repeatability of test results as two specimens can be produced from a single disk from the compacted sample or field cores, thus increasing the number of specimens per sample. Given its advantages, SCB has been used to test fracture resistance of AC mixtures albeit with different test conditions and parameters without much knowledge on how the test conditions affect the repeatability of the results. The objective of this chapter is to develop the SCB test method based on an integrated experimental-statistical approach that considers critical test parameters to provide repeatability and practicality.

3.2 SCB Sample Preparation



(a)



(b)

Figure 7. Mixture collection: (a) from a mixture delivery truck and (b) containers of mixtures.

To prepare SCB samples, AC mixtures were collected from plant/field prior to paving (Figure 7a) and transported in sealed containers (to avoid aging by oxidation) to the testing laboratory (Figure 7b). The mixtures were then heated respective recommended compaction temperature (e.g., 150°C) for a minimum of two hours. During oven heating, the mixture was intermittently disturbed during heating (e.g., every 30 minutes) using a spatula to ensure homogenous heating throughout. The purpose of heating is to increase the workability of the mixture and facilitate compaction by SGC (Superpave gyratory compactor).

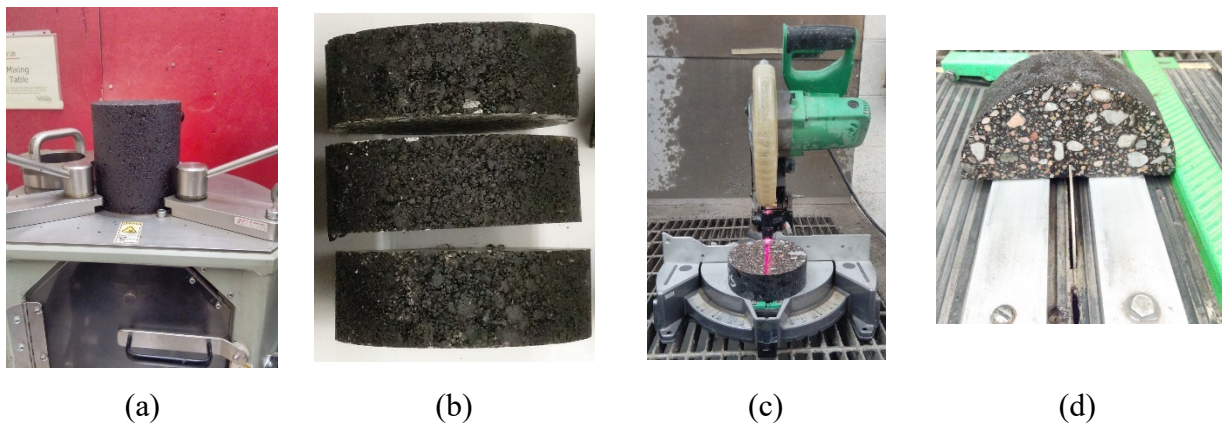


Figure 8. SCB sample preparation: (a) compaction by SGC , (b) slicing, (c) halving and (d) notching

The loose mixtures were then compacted using the SGC (Superpave gyratory compactor) to form a tall sample of 170 mm in height and 150 mm in diameter (Figure 8a). The tall specimens were compacted at target air voids of $4 \pm 0.5\%$. The compacted sample was then sliced into discs at a desired thickness after discarding the top and bottom 10 mm discs of the sample (Figure 8b). Subsequently, the discs were halved into semi-circulars (Figure 8c) onto which a notch of desired length was introduced (Figure 8d). Water was used during the fabrication process to cool specimens and neutralize dust generated during cutting/slicing the AC. Subsequently, SCB specimens are left to dry in front of a fan for 24 hours at room temperature.

3.3 SCB Test Set up and Data Analysis

Figure 9(a) shows the test set-up of SCB in which specimen with a diameter of 150 mm is loaded from the top-center at using (LPD) load-point displacement. The span length for all specimens

here-in was selected to be 0.8 diameter which is 120 mm. A notch with length nl is introduced at the bottom-center of SCB specimen to initiate fracture since the main objective of the SCB test is to characterize the propagation of cracks rather than their initiation. Figure 9(b) shows a full propagated crack at the end SCB fracture test of an AC mixture. Note that placing the notch in the center of span the resulting fracture was parallel to the notch resulting in mode I fracture which is the focus of this study.

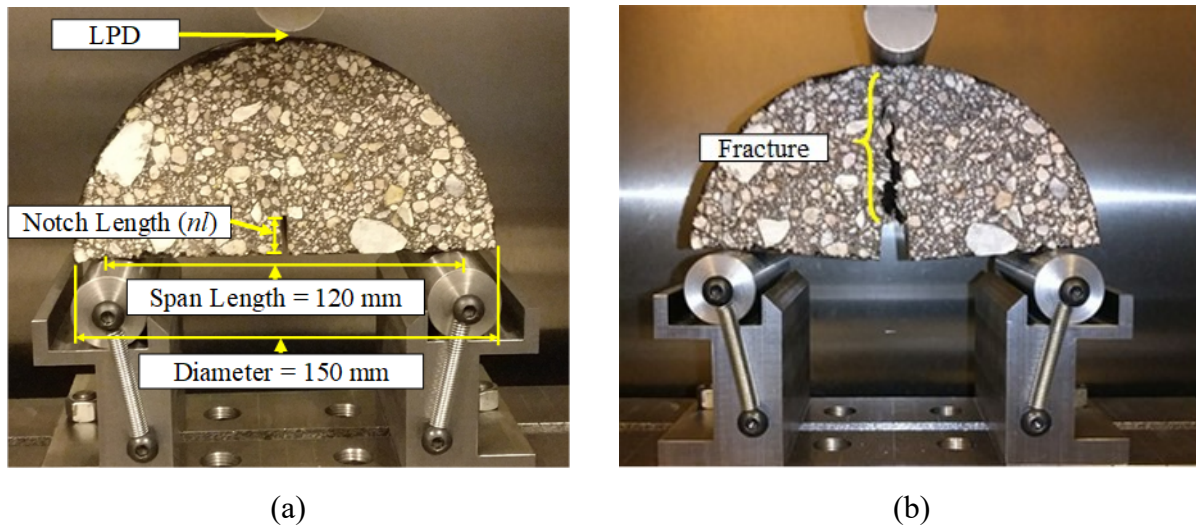


Figure 9. SCB fracture test: (a) test set-up and (b) fracture after SCB testing.

During the test, load and load-point displacement (LPD) were measured and recorded by the data acquisition system. Specifically, this study used a UTM-25kN load machine fitted with a 25kN load cell, an environmental chamber capable of -16°C to 60°C and a computer-controlled CDAS (central data acquisition system).

Typical SCB test results are shown in Figure 10 with applied data analysis. Work (W) is defined as the area underneath the load-LPD curve calculated by numerically integrating a fitted function to the results (Figure 10). In this study, all SCB data were fitted with eight Gaussian functions [47]. Fitting the curve allows for identification of other curve-derived variables such as: the maximum load (i.e., peak load or P_{max}), pre-peak (m_1), post-peak (m_2) slopes, and critical displacement. It is noteworthy that the post-peak slope (m_2) is calculated at the inflection point of the fitted function after numerical differentiation.

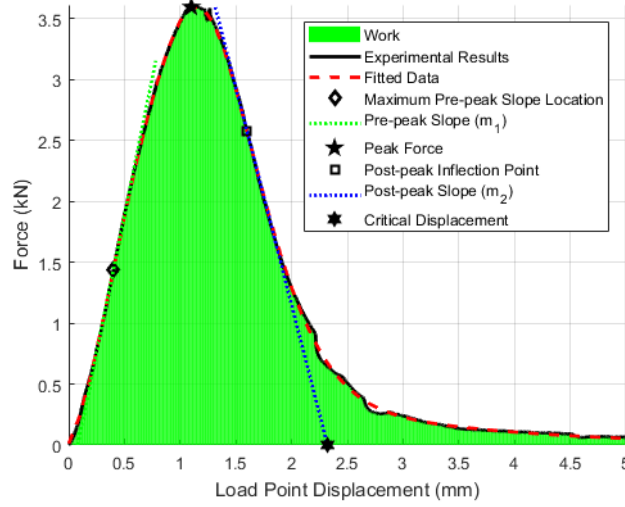


Figure 10. SCB test results and analysis.

From the test results in Figure 10, several fracture-related indicators such as Fracture energy (G_f) is calculated per Equation 1 by normalizing work (W) to the ligament area (A_{lig}).

$$G_f = \frac{W}{A_{lig}} \quad \text{Equation 1}$$

where $A_{lig} = t \times (R - nl)$ and b , R and nl are the specimen thickness, radius, and notch length.

The flexibility index developed by Ozer, Al-Qadi [48] can also be calculated from the test results using Equation 2 as such:

$$FI = \frac{G_f}{|m_2|} \times 10 \quad \text{Equation 2}$$

where G_f is expressed in kJ/m^2 and the post-peak slope at the inflection point, m_2 , is expressed in kN/mm . As the above equation indicates, FI considers the speed at which damage occurs by incorporating the post-peak (m_2) slope. It is noted that, during SCB testing, damage due to cracking occurs immediately after the maximum load and is characterized by a continuous reduction of the load-bearing capacity of the specimen as the crack propagates until complete failure.

The cracking resistance index recently developed by Kaseer, Yin [49] as another fracture-related indicator calculated from SCB results per Equation 3:

$$CRI = \frac{G_f}{P_{max}} \quad \text{Equation 3}$$

Fracture energy was used in the subsequent development of the SCB test method since most of the indicators stated above are based on fracture energy. As such, repeatability of G_f will propagate to the other derived indicators.

3.4 Testing Variables

3.4.1 *Methodology*

The testing parameters are the minimum recommended number of specimens (n), specimen thickness (t), notch length (nl), loading rate (lr), and the testing temperature (T). In addition, the testing fixtures will also be investigated for their effects on test results and their repeatability. An extensive literature review was conducted to serve as the starting point to the testing variables which were determined concurrently as follows: first, a reasonably large sample of SCB specimens (e.g., 18) was tested using testing variables from the literature review to determine the recommended number of replicates for SCB. Second, using the determined number of replicates, SCB test specimens were tested at varying thicknesses (e.g., 25 – 60 mm) to select specimen thickness based on repeatability (i.e., coefficient of variation) and practicality. Third, the determined n and t , several specimens were prepared at different notch lengths (i.e., 0 – 40 mm) to select a nl based on observed repeatability and practicality. The loading rate was also investigated by considering the previously determined testing variables (i.e., n , t , nl) on SCB specimens at different loading rates. The lr was then selected considering practicality and repeatability. Finally, the testing temperature was investigated using pre-determined n , t , nl , and lr at different temperatures.

3.4.2 *Materials*

A typical Nebraska mixture, SPH, was selected for the SCB test method development effort. The mixture is mainly used on important roads (e.g., interstate) due to its high quality (i.e., better grade binder and a good source of aggregates). The materials were collected just as the truck was leaving the plant heading to the field (Figure 7a). Sealed containers were used to transport and store mixtures to avoid undesired aging due to oxidation before sample fabrication (Figure 7b). The mixture was compacted after two hours of oven heating at the specified compaction temperature of 300°F (149°C).

3.4.3 Results and Discussion

3.4.3.1 Number of Replicates

Using the testing variables found in the literature, 18 specimens were prepared and tested at $t = 50 \text{ mm}$, $nl = 15 \text{ mm}$, $lr = 1 \text{ mm/min}$ and $T = 21^\circ\text{C}$ [50-54]. By testing a large enough sample size, the inference of the recommended minimum number of specimens could be made with reasonably good accuracy. Due to the heterogeneous nature of AC mixtures, the number of specimens is critical in ensuring the reliability of test results. As such, the first effort of the SCB test development effort was to find the necessary number replicates within a statistical significance.

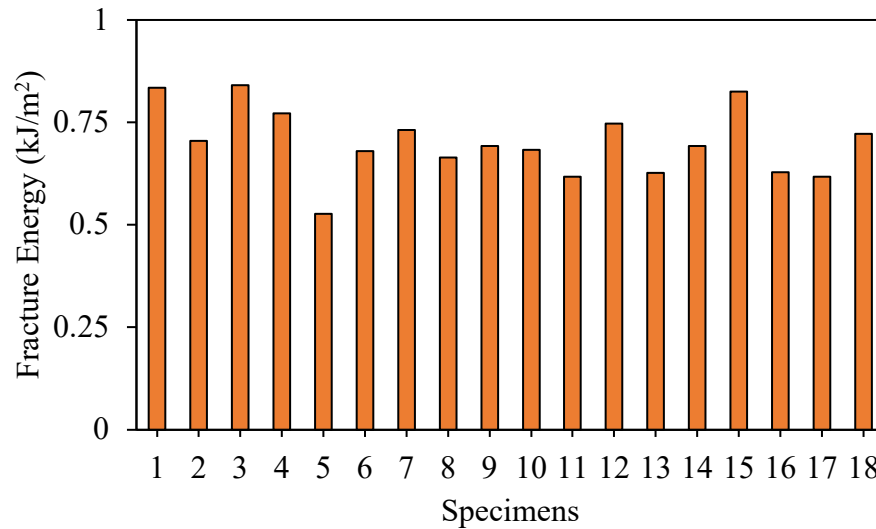


Figure 4 Test results for the sample used to determine minimum number of replicates

The recommended minimum number of replicates was calculated using Equation 4 which assumes a normal distribution of the results [47]. A normality check was then conducted to ensure that the results can be treated as originating from a normal distribution.

$$n = \left[\frac{Z_{\alpha/2} \times \sigma}{E} \right]^2 \quad \text{Equation 4}$$

where E is the margin of error, $Z_{\alpha/2}$ is the standard normal deviate at a given probability level α (e.g., 5% in this study) and σ is the sample standard deviation. The margin of error is simply the

difference between the observed sample mean (\bar{y}) and the true value of the population mean (μ) as such: $E = \bar{y} - \mu$.

As Equation 4 assumes a normal distribution of the sample data, a normality check of the G_f from the 18 specimens was conducted following [55, 56]. The normality test is also commonly known as the Lilliefors test.

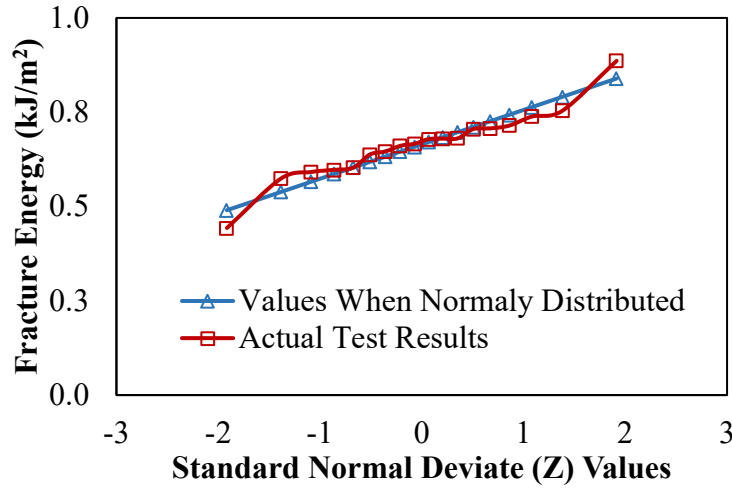
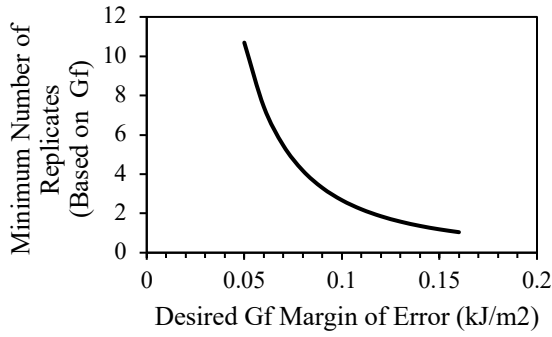
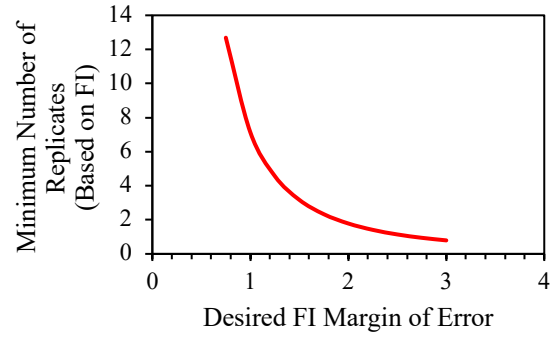


Figure 5. Normality check of the sample

Figure 5 shows the test results as compared to results from a normal distribution of the same standard deviation and mean, which are the two parameters that are needed to fully define a normal distribution. Both distributions shown in Figure 5 were statistically compared using the Chi-square and found statistically similar at $\alpha = 5\%$ (i.e., $\chi^2 = 0.016 \leq \chi^2_{0.10,17} = 27.587$). As a result, fracture energy of the 18 specimens was taken to be of a normal distribution which allowed the use of the Equation 4 to determine the recommended number of replicates. Figure 6 shows the different recommended minimum numbers of replicates per the margin of errors of both G_f and FI . The probability level α was 5% which corresponded to $Z_{\alpha/2} = 1.96$. The average and the standard deviation for G_f calculated were 0.7 kJ/m^2 and 0.0834 kJ/m^2 , respectively. To determine the recommended n , a margin of error (E) equal to 0.07 kJ/m^2 , which is 10% of the average G_f , was selected as a threshold to calculate the minimum recommended number of replicates $n \approx 5.34$. Therefore, a minimum of five to six replicates is recommended when conducting the SCB test.



(a)



(b)

Figure 6. The minimum number of replicates versus the desired margin of error: (a) based on fracture energy, Gf, and (b) based on the flexibility index, FI.

3.4.3.2 Thickness

Four thicknesses: 30, 40, 50, and 60 mm were investigated. Six specimens per each thickness were prepared are recommended from the previous section. Figure 7 shows the SCB test results at the different thicknesses in which the maximum load increased with thicknesses. In addition, results curves from smaller thicknesses showed varying levels of noise suggesting their insufficiencies.

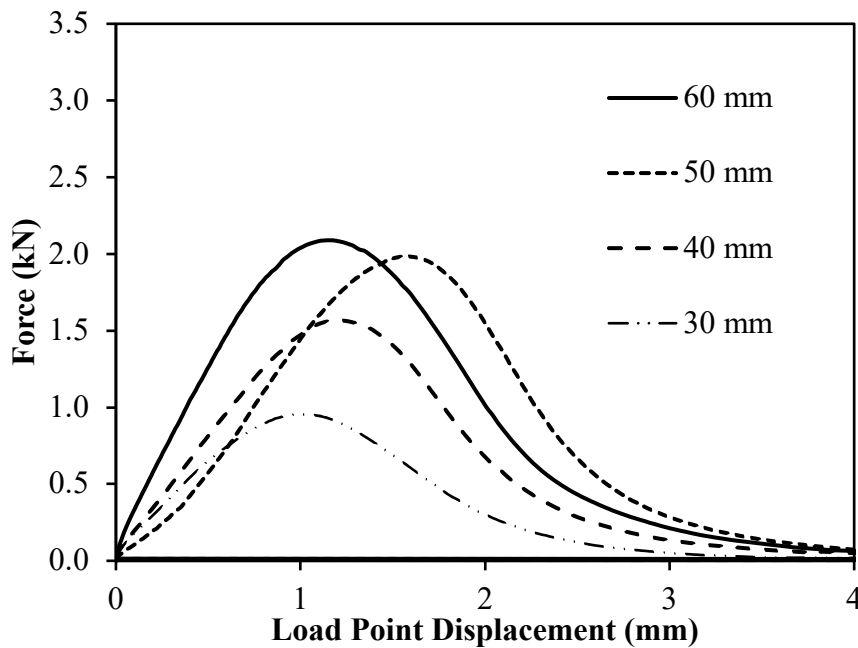
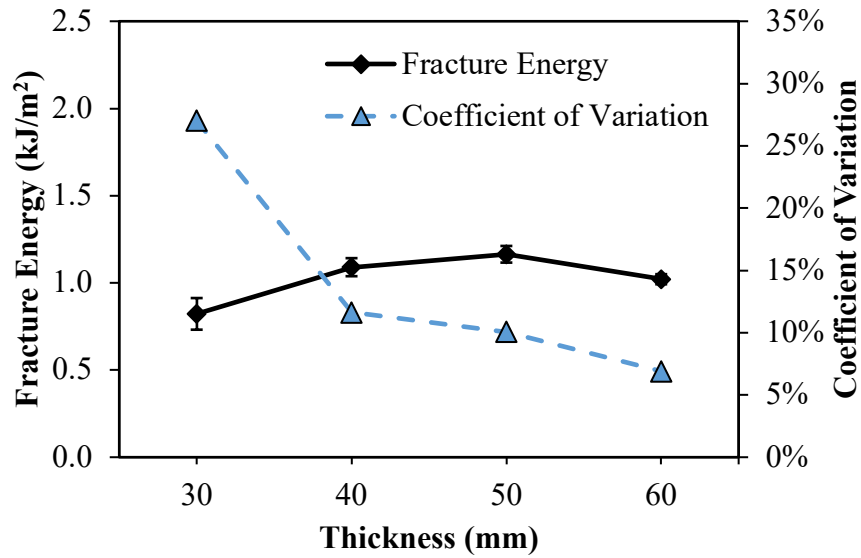


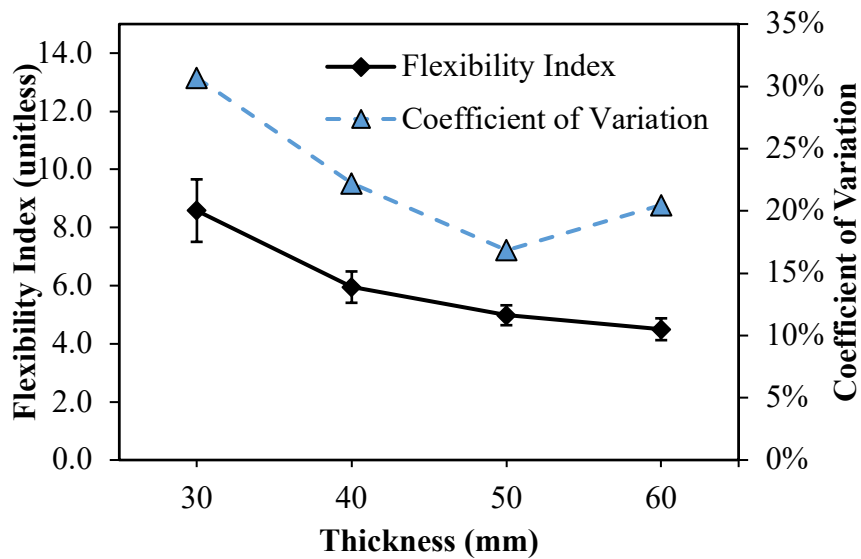
Figure 7. SCB test results at different thicknesses.

Analysis of the test results from Figure 7(a) is shown in Figure 8 where the fracture energy was calculated along with associated COV (coefficient of variation). It noteworthy that COV is the standard deviation normalized to mean [47]. The analysis results showed that G_f initially increased with thickness up until 50 mm, beyond which is reduced. In addition, COV results show that increasing thickness benefitted repeatability. However, beyond 40 mm thickness, the improvement in repeatability was minimal. As a result, an SCB thickness of 40 mm or higher was recommended as shown in Figure 8 in the green region.

The analysis also indicates that FI values are reduced with increasing thickness until 50 mm (Figure 7(b)). Beyond 50 mm, the FI continued to decrease, however, its COV increased. This indicates that a thickness of 50 mm provides the optimal repeatability of both G_f and FI when conducting the SCB test. Therefore, a thickness of 50 mm was recommended and selected for the next steps based on the overall low COV of both G_f and FI . The thickness of 50 mm agrees well with the previous studies by Wittmann and Zhong [57], Brühwiler, Wang [58] indicating that the thickness of AC specimens should be at least four times larger (i.e., 12.5 mm $\times 4 = 50$ mm) than NMA size (12.5 mm in this study)



(a)



(b)

Figure 8. Effect of specimen thickness on test results and their repeatability: (a) fracture energy and (b) flexibility index.

3.4.3.3 Notch Length

Four different notch lengths (5, 15, 25, 40 mm) and one notch-less (i.e. 0 mm) were investigated. Six specimen of 50 mm thickness were tested per each notch length. The results are shown in Figure 9 and they indicate inverse proportionality of load and notch length. In addition, location of P_{max} shifted to the right unlike in for thickness (Figure 7).

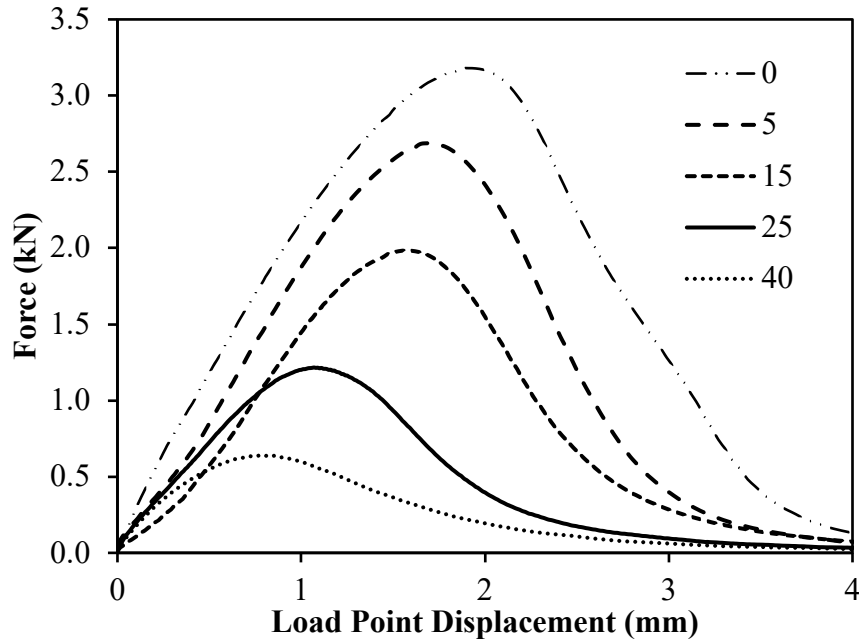


Figure 9. SCB test results at varying notch lengths.

The results are reasonable since a smaller notch allows for more ligament area thus more load-resisting materials resulting in increased force at a given LPD.

Figure 10 shows the analysis of test results (from Figure 9) at varying notch lengths. The results show that the fracture energy (G_f) generally decreased with increasing notch length with the sharpest drop happening for notches longer than 15 mm. An interesting observation is that the notch length of 5 and 15 mm produced virtually similar G_f values. However, the COV results show that the 5 mm notch had the lowest value of approximately 10%, while the remaining notches had similar values of approximately 15% (Figure 10 (a)). Repeatability results in terms of COV show that lack of notch ($nl = 0$ mm) and too long notch ($nl = 40$ mm) increased COV. The high COV from the notch-less specimens can be explained by random crack initiations from off-center as shown in Figure 11. Without notch, different specimens will have different locations from which crack will initiate resulting in widely variable ligament area and fracture energy thus the high COV. However, as soon as the notch is introduced to the specimen (e.g., $nl = 5$ mm) the COV quickly drops as all cracks initiate from the same location in the specimen. The COV stays low but slowly increases until $nl = 25$ mm. At $nl = 40$ mm, COV spikes again, which indicates another source of variation in the results. A possible explanation is that as the notch length increases beyond a certain

point, the ligament area reduces past the intrinsic RVE (representative volumetric element)[59, 60]. Approximately RVE is about four times the MAS (maximum aggregate size) which in this case is 12.5 mm resulting in an RVE of 50 mm. Consequently, $nl = 40$ mm resulted in only ligament are of $35 \text{ mm} \leq \text{RVE}$ thus the increased COV. Based on the repeatability results, a notch length between 5 and 25 mm is recommended for the SCB testing method as shown in Figure 10 in the green region.

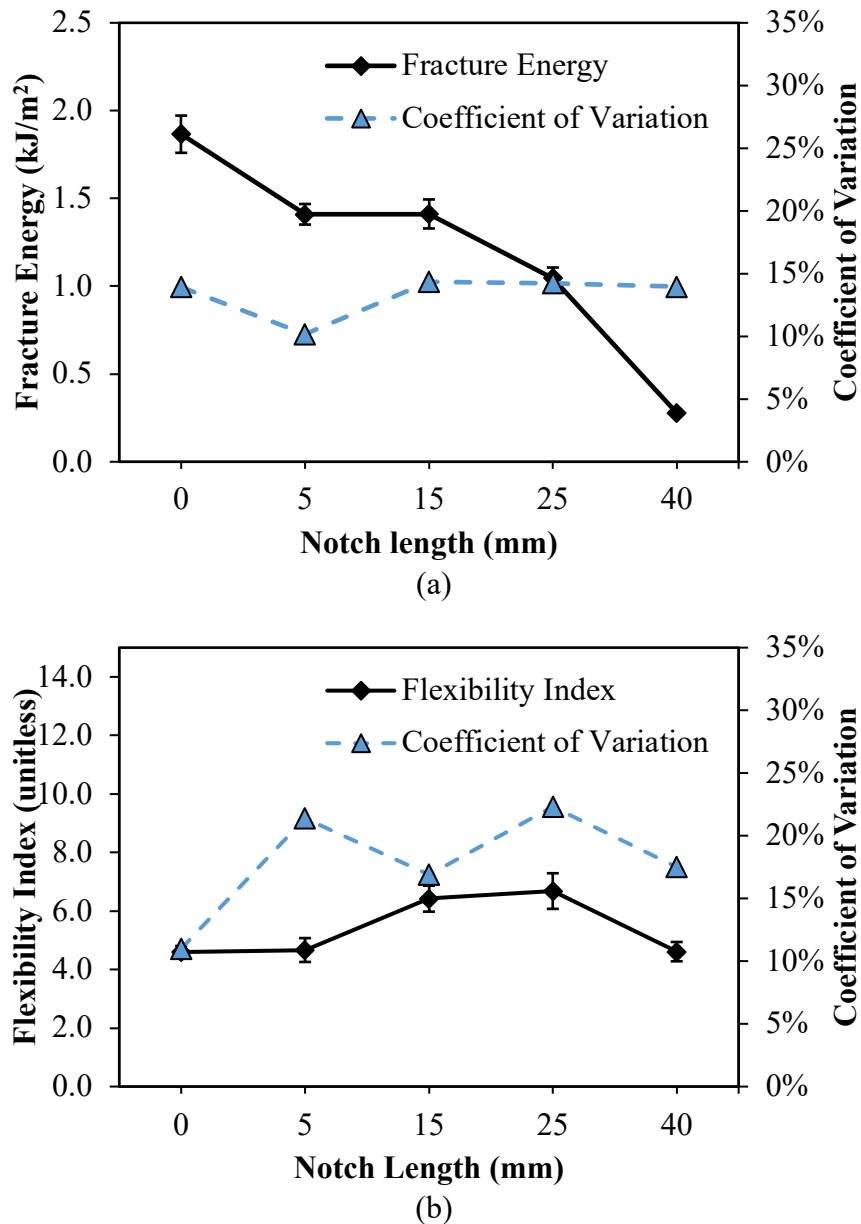


Figure 10. Effect of notch length on test results and their repeatability: (a) fracture energy and (b) flexibility index.

The effects notch length to the FI results and their repeatability in terms of COV are shown in Figure 10 (b). Unlike for G_f , the FI results remained relatively similar at the different notch lengths, suggesting reduced sensitivity of FI to the notch variation when compared to G_f . Therefore, in the case where notch length manufacturing is an issue, FI would yield more consistent results. However, as seen in the same figure, the COV of FI at the notch lengths generally higher than for COV of G_f . The lowest COV of FI can be found on notch-less (i.e., 0 mm) specimens while the highest is found on 25 mm long notches. Notch-less specimens are undesired since they produce off-centered cracks that are not consistent with the mode-I fracture (Figure 11). With consideration of the respective repeatabilities of both G_f and FI , the notch length of 15 mm was selected for the next steps.



Figure 11. Off-center crack initiation for notch-less SCB specimens.

3.4.3.4 Loading Rate

Considering the previous recommendations of SCB testing variables, four loading rates (e.g., $lr = 0.1mm/min$, $0.5mm/min$, $1mm/min$, $5mm/min$ and $10mm/min$) were investigated at $n = 6$, $t = 50mm$ and $nl = 15mm$. Figure 19 shows test results at the different loading rates in which faster rates produced higher load from the SCB specimens. Since AC mixtures are considered to be viscoelastic [61-64], an increase in the rate of loading thus straining, will result in increased resisting stress in mixtures due to viscosity [65] which translated into higher reaction forces as reflected in Figure 19.

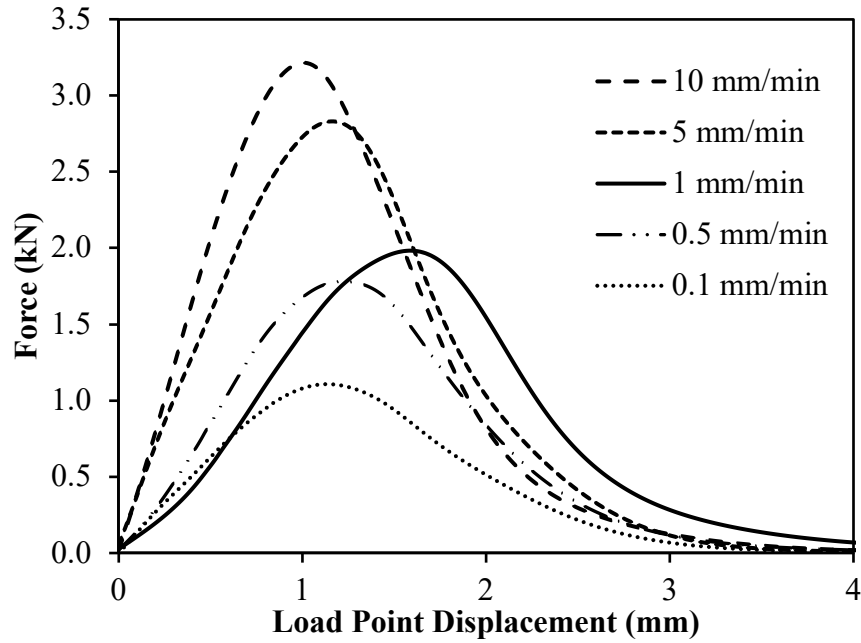
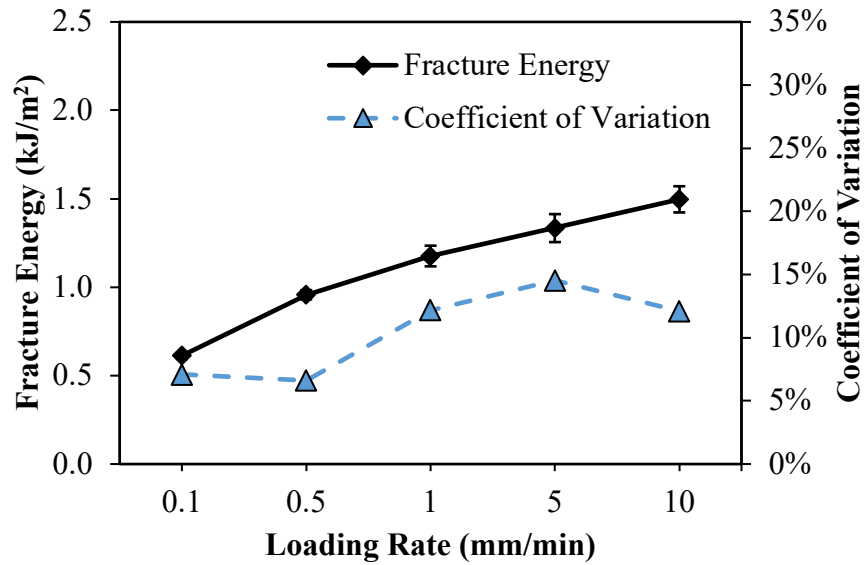
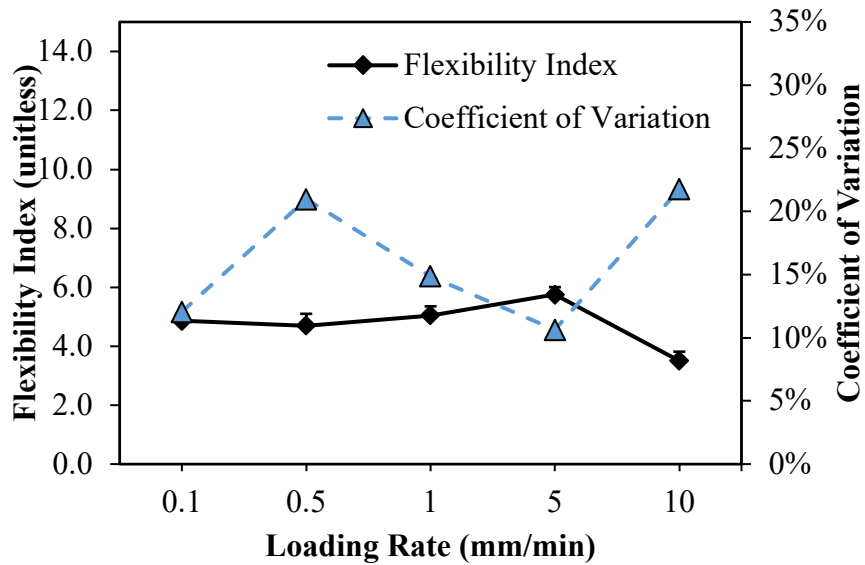


Figure 19. SCB test results at different loading rates.

Results shown in Figure 12(a) indicate that the loading rate had minimal effect on both fracture energy and associated COV compared to other testing variables (e.g., t and nl). In fact, G_f only fluctuated between 1.03 kJ/m² at 0.5 mm/min and 1.4 kJ/m² at 10 mm/min, which is a much narrower range compared to the effects of t and nl on G_f (Figure 8 and Figure 10).



(a)



(b)

Figure 12. Effect of loading rate on test results and their repeatability: (a) fracture energy and (b) flexibility index.

Similar to G_f , COV (of G_f) results were minimally affected by the loading rate within the range tested. COV generally stayed just below 10% and increased to slightly above 12% at 5 and 10 mm/min loading rates. For repeatability purposes, the loading rate can be considered to have minimal effect on results while for practicality purposes, a slower loading rate may not be recommended. As a result, loading rates between 1-5 mm/min can be recommended mainly

because within the range, G_f stabilized and COV only varied from 9.5% to 12%. A COV of G_f lower than 25% is considered indicative of satisfactory repeatability [40]. In the subsequent investigations, a rounded average of the recommended range (i.e., 3mm/min) was used.

Figure 12(b) shows the results of FI and its repeatability at different loading rates. The FI results were minimally affected by the loading rates up until 5 mm/min rate, beyond which the FI dropped by almost 50% (halved). The reduced sensitivity of the FI over the wide range (i.e., 0.1 to 5 mm/min) suggests that FI results from this range can directly be compared with each other. The suggestion warrants further investigation, which is out of the scope of this study. COV of FI varied with loading rate with the rates of 0.1 and 5 mm/min having the lowest values. It should be noted that beyond 5 mm/min, FI COV seemed to start increasing and would likely keep increasing. As aforementioned, with increasing loading rate asphalt mixtures become stiffer and therefore more brittle. Brittle specimens break suddenly and make it difficult to obtain the post-peak slope (m_2) needed to calculate FI and thus increase in variability (i.e., COV).

In sum, the SCB loading rate has minimal effect on FI results and linearly increase with G_f . The COV of FI is more sensitive to varying loading rates compared to COV of G_f . Although a slow loading rate (e.g., 0.1 mm/min) yields repeatable results, it significantly reduces practicality due to the considerable increase in testing time. As a result, loading rates between 1-5 mm/min are recommended mainly because within the range, COV of G_f and FI varied only within 10% to 15%. A COV of G_f lower than 25% is considered indicative of satisfactory repeatability [40].

3.4.3.5 Temperature

Three temperatures (15°C, 21°C and 40°C) were investigated at the predetermined recommended testing variables (i.e., $n = 6$, $t = 50mm$, $nl = 15mm$, and $lr = 3mm$). It should be noted that the rationale of selecting the intermediate to high temperature was to investigate the effect of temperature on SCB test results in a wider range of potential fatigue cracking. Figure 13 shows the SCB test results of the different temperature where the maximum load (P_{max}) increased with decreasing temperature. As aforementioned, AC mixtures are viscoelastic, and as such, they are time and temperature-dependent. The low temperature will result in stiffer mixtures manifested as a higher P_{max} and pre-peak slope (m_1). Conversely, increased temperature resulted in soft, more

compliant mixtures which reduced the P_{max} and m_1 . Comparing Figure 19 to Figure 13, it becomes apparent that increasing temperature has a similar effect as lowering the loading rate. This is a core characteristic of viscoelastic materials that allow time-temperature superposition depending on rheological classification (e.g., simple or complex) of the material [65].

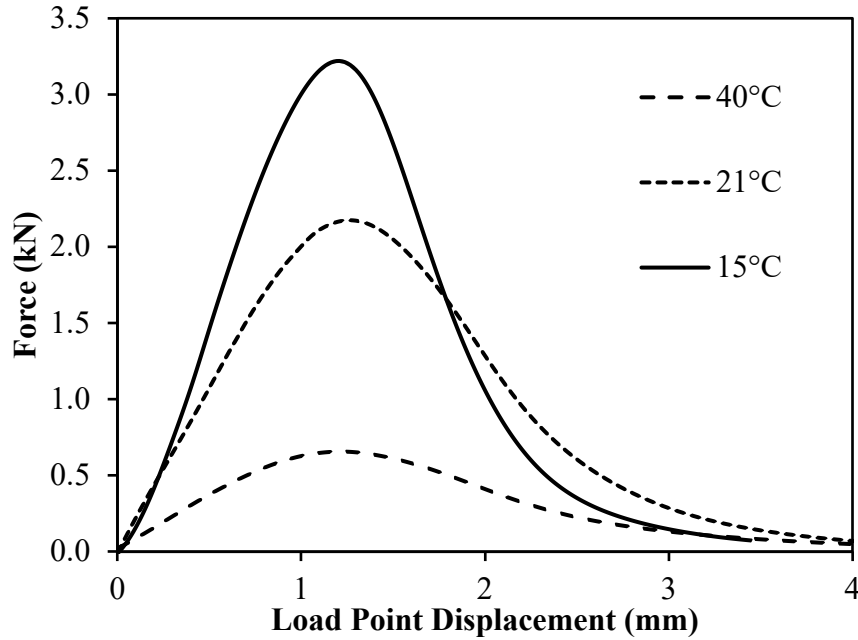
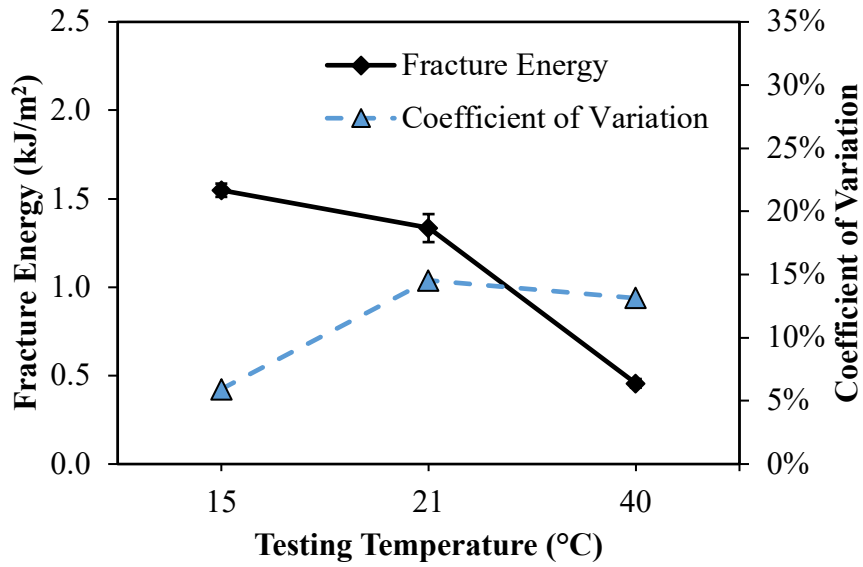
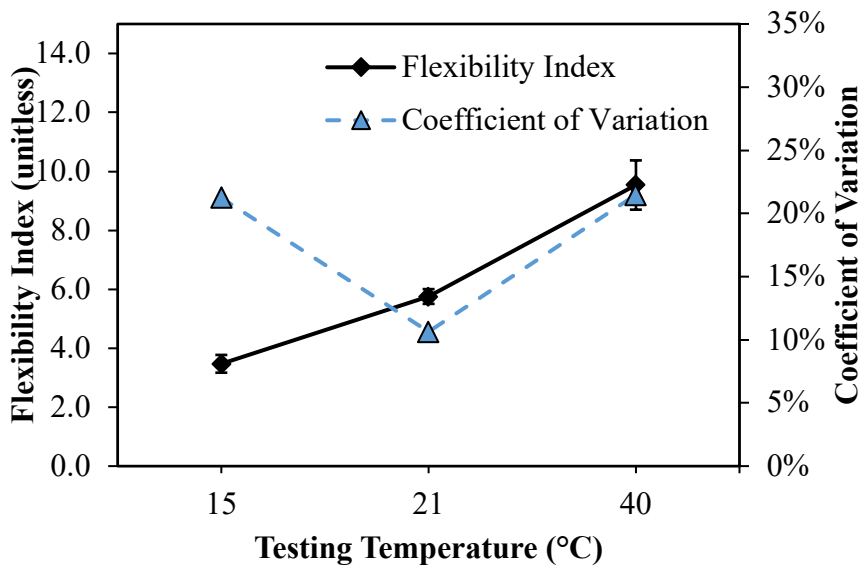


Figure 13. SCB test results at different temperatures.

Figure 14(a) shows results when temperatures varied. Generally, the fracture energy decreased with increasing temperature. This is reasonable since the area underneath the curve decreased with temperature (T) as shown in Figure 13. However, this decrease of G_f with increasing T was relatively less pronounced between temperature range of 15°C and 21°C compared to the range of 21°C and 40°C. Continually increasing temperature would eventually result in a too soft mixture, which would collapse at the slight application of force and thus untestable for fracture. The high temperature is mainly reserved for rutting (permanent deformation) testing of mixtures. For the fracture testing in AC mixtures, high temperatures are usually avoided due to the increased compliance.



(a)



(b)

Figure 14. Effect of testing temperature on test results and their repeatability: (a) fracture energy and (b) flexibility index.

Repeatability of G_f results show increased COV with increasing temperature from 5% at 15°C to 13% at 40°C (double fold increase). As aforementioned, high temperature resulted in increased compliance which diluted the fracture test results. This is because the main mixture failure phenomenon was by deformation rather than fracture. However, it is noted that, within the temperature range tested, COV remained satisfactorily with lower than 25% which is considered

an acceptable repeatability in SCB G_f results [40]. Based on practicality and repeatability, a room temperature of 23°C can be recommended for SCB. This can eliminate the need for environmental conditioning equipment.

The effect of temperature on FI is presented in (Figure 14(b)) where the FI increased with increasing temperature. This is reasonable since FI is obtained by dividing the G_f to the post-peak slope. As can be seen in Figure 13, higher temperature SCB test results produce more compliant post-peak slope (m_2). Apparently, although G_f reduces with increasing temperature, the post-peak effect is dominant in the calculation of FI .

COV of FI show an initial decrease between the temperature range of 15°C to 21°C, after which the COV value sharply increased. It is as though the low temperature increases the variability of FI due to the aforementioned brittleness behavior that complicates the calculation of post-peak slope (m_2). Similarly, the higher temperature seems to have increased the variability of FI since the mixture became more compliant and thus more likely to vary. Ultimately, considering the results and repeatability of G_f and FI , a temperature of 21°C is recommended for SCB testing. The 21°C temperature has an added advantage of being the typical room temperature and thus, eliminates the need for an expensive environmental chamber and therefore increasing the practicality of the SCB test method.

3.5 Testing Fixtures

Although SCB testing variables are critical in ensuring repeatability of the test results, equally important are the fixtures used in conducting the test. Understanding the effect of load-support fixtures on SCB test results is important towards wide adoption of the test by state departments of transportation (DOTs) as a tool for QC/QA. This is because when SCB is widely adopted, it may be performed using readily available load-support fixtures which may not be identical between laboratories. Consequently, due to the different fixtures, varying SCB results may be obtained despite similar testing variables (e.g., n , t , nl , lr , and T). In addition, repeatability of the test results could also be fixture dependent which, if not taken into consideration, may dilute the statistical significance of the results.

A possibility then arises that results from different DOTs or laboratories that used different load-support fixtures cannot be directly compared in a statistically meaningful manner. Thus, to

ensure the quality of the results towards more consistent implementation of the SCB test method, it is necessary to investigate how the different load-support fixtures frequently used for SCB testing influence test results and testing repeatability. Specifically, this second part of SCB test development will focus on: 1) effects of load-support fixtures on SCB test results and their repeatability; and 2) effects of predominant SCB testing fixtures on test results (i.e., fracture energy, flexibility index, etc.).

3.5.1 Materials

A typical Nebraska dense-graded AC mixture was selected for this examination and was collected from a construction site just before paving. This mixture, which is typically used on high traffic volume roads, was transported in sealed containers to avoid aging by oxidation. The aggregate gradation of the mixture and the corresponding blending proportions are shown in Table 1. Aggregate properties of the entire blend, which was composed of 32% recycled asphalt pavement (RAP), are given. The total binder content, which includes recycled binder from RAP, was 5.20% of the total mixture weight.

TABLE 1 Aggregate Gradation and Properties

Aggregate	%	Aggregate Gradation (% Passing on Each Sieve)									Binder PG 64-34
		19mm	12.5mm	9.5mm	#4	#8	#16	#30	#50	#200	
¾" CHIPS	10	100	60	18	2.0	2.0	1.0	1.0	1.0	1.0	5.2%
CR. Gravel	53	100	100	100	92.7	73	45.2	29.1	16.2	6.3	
2A Gravel	5	100	95.4	90.9	68	27.3	8.6	3.5	1.1	0.2	
Millings	32	100	94	90	68	41	29	23	19	8	
Combined	100	100	93.9	88.1	74.5	53.4	33.8	23.1	14.8	6	
Aggregate Properties											
FAA	CAA	SE	F&E	D/B	G _{sb}						
45	99/96	79	0.1	1.18	2.585						

FAA: Fine aggregates angularity; CAA: Coarse aggregates angularity; SE: Sand equivalent
F&E: Flat and elongated particles; D/B: Dust to Binder Ratio; G_{sb}: Bulk specific gravity.

To fabricate SCB specimens, the AC mixture was heated at the recommended compaction temperature of 150°C for two hours and then compacted into tall SGC samples of 170 mm in height and 150 mm in diameter targeting air void of 4.0% by volume. Based on the recommendations from the previous section, the testing variables were selected as such: thickness (t) = 50 mm, notch length (nl) = 15 mm, loading rate (lr) = 3 mm/min and temperature (T) $23 \pm 0.5^\circ\text{C}$.

3.5.2 Methodology

To meet the objectives stated above, six different configurations of SCB load-support fixtures were identified and investigated. All fixtures were assigned to SCB specimens fabricated from the same AC mixture and tested under identical conditions. Consistent sample preparation was achieved by dedicating a single working day to each sample preparation step (i.e., compaction, cutting, testing). Eight SCB replicates per fixture were tested, which was more than the minimum number of replicates (six) recommended in the previous section. However, since the scope of this effort involves multiple fixtures, which may bring a greater level of variability, the sample size was conservatively increased. Testing fixtures were selected to include key components of fixtures such as: rolling freedom, shape of rolling, and presence of mid-span jig on test results. Figure 15 presents the nomenclature used to describe each testing fixture.

3.5.3 Configurations of Test Fixtures

As shown in Figure 15, each fixture component is composed of specific descriptions. For example, the rolling freedom component have the following descriptions: free, spring, and restricted. When nothing is inhibiting free rolling the support rollers, the rolling freedom is free [66, 67]. In contrast, if the rollers cannot move horizontally while rotating, the rolling freedom is restricted [68-70]. Finally, if a spring is used to retain the rollers from moving too far from initial positions then the rolling freedom is named spring. It is noteworthy that the roller springs used in here had a typical spring constant of 0.12 N/mm [44].

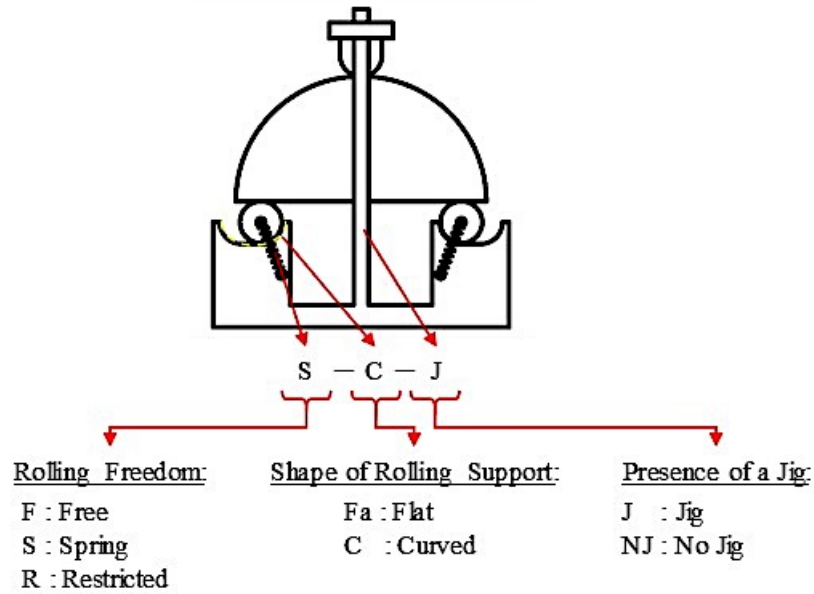
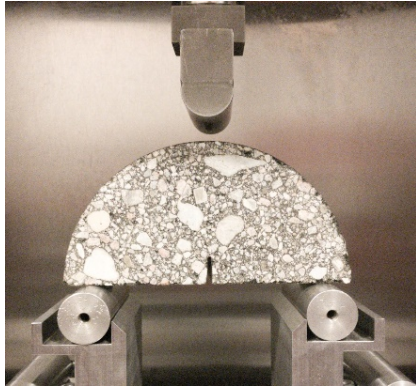
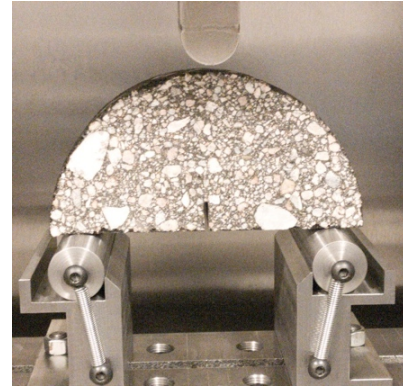


Figure 15. The nomenclature used on SCB test fixtures.

The shape of rolling support has two descriptions: flat or curved which, simply describes the shape on which the support rollers are placed and thus will be rolling. Both flat and curved shapes have been used by several studies without insight on how these surfaces affect the results. The last fixture component was the mid-span jig and which have been implemented on commercial SCB testing load frames such as Auto_SCB™ that NDOT acquired. It is, therefore, necessary to understand the effects of the presence of the jig on test results before being deployed by NDOT.



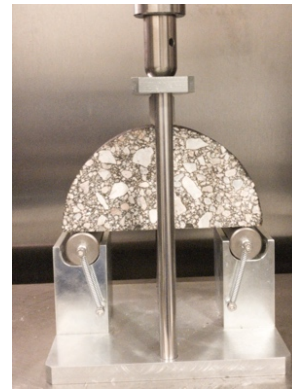
F-Fa-NJ [66, 67]



S-Fa-NJ



F-C-J



S-C-J



S-C-NJ



R-C-NJ [68-70]

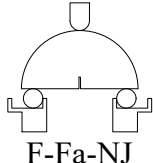
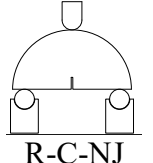
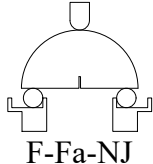
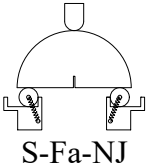
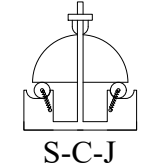
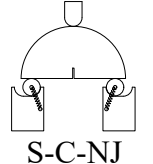
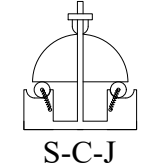
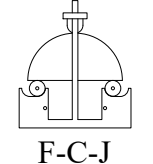
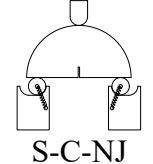
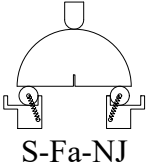
Figure 16. Configurations of investigated SCB load-support fixtures.

3.5.4 *Pairwise Comparison of Fixtures*

Six testing configurations selected for fixture study effort are shown in Figure 16. Fixtures were selected to provide helpful insight on how each component affects the SCB test results by using a simple comparison. For example, comparing F-C-J with S-C-J, one can deduce the effect of having

a roller spring on a curved rolling surface. Similarly comparing results from S-Fa-NJ with F-Fa-NJ one can also infer the effect of roller springs on a flat rolling surface. A complete comparison process to extract the effect of each component is shown in Table 2.

Table 2. Comparison process to extract the effect of fixtures components

Fixtures comparison		Comparison result		
 F-Fa-NJ	vs.	 R-C-NJ	→	Effect of free rolling at support
 F-Fa-NJ	vs.	 S-Fa-NJ	→	Effect of roller springs on a flat rolling surface
 S-C-J	vs.	 S-C-NJ	→	Effect of mid-span jig
 S-C-J	vs.	 F-C-J	→	Effect of roller springs on a curved rolling surface
 S-C-NJ	vs.	 S-Fa-NJ	→	Effect of rolling surface shape

All tests in Table 2 were performed using identical testing conditions. Data were analyzed to determine several fracture-related indicators, and the coefficient of variation (COV) values were calculated to examine testing repeatability. Results were interpreted to characterize the contribution of individual fixture components to the variability (or repeatability) of test results.

3.5.5 Assigning Specimen to Fixtures

The process of fabrication of SCB specimens involves compaction of a 170 mm tall and 150 mm diameter AC samples by the Superpave Gyratory Compactor (SGC). Previous studies [48, 71] have demonstrated the existence of non-uniform air void distribution within the SGC compacted

tall samples with the relatively higher air void content located towards the outer surface of the sample. Thus, even though the bulk air voids of tall specimens were measured, different levels of air could be introduced into specific areas of each tall sample [71] which would contribute to sample-to-sample variability. To reduce the inevitable location-specific variability, when assigning specimens to a testing case, the scheme shown in Figure 17 was implemented to improve the distribution of specimens. In addition, higher air void containing top and bottom 10 mm disks were trimmed and discarded from tall SGC samples before proceeding with fabrication of SCB specimens.

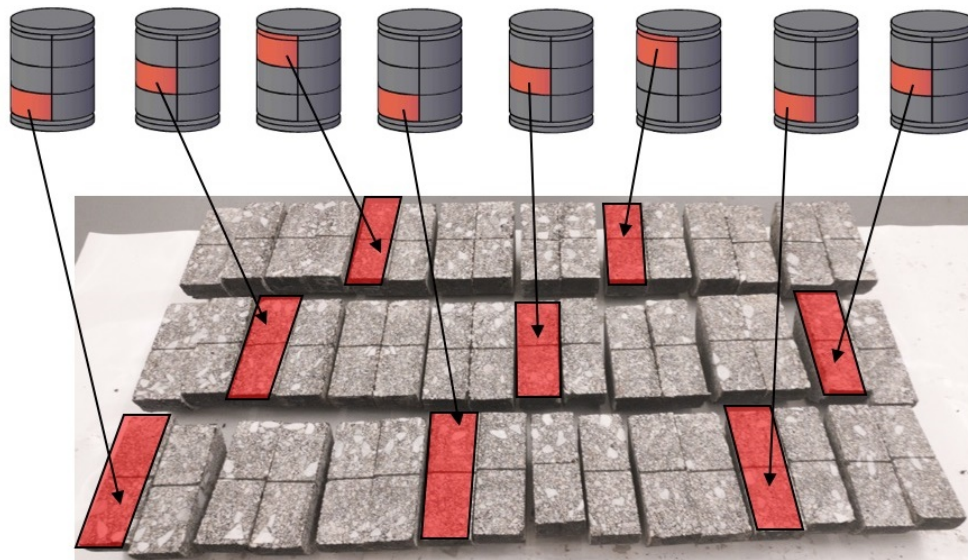


Figure 17. Scheme to reduce location-specific variability of SCB testing specimens.

3.5.6 Results and Discussion

SCB test results from all fixtures are shown in Figure 26 for the eight replicates. From the results, it is apparent that fixtures with a jig (i.e., S-C-J and S-C-J) tended to produce curves within a relatively narrower band compared to other fixtures. Another observation is that combination of spring rollers and jig considerably narrowed the band of curves in the pre-peak region for the S-C-J fixture suggesting existence constrain on SCB specimen when the fixture is used. The jig effect especially apparent by comparing test results from S-C-NJ and S-C-J where the jig indeed did narrow the band of results curves.

When the free horizontal rolling was restricted as is the case for R-C-NJ, the maximum load was highest among all fixtures investigated. The high P_{max} of R-C-NJ can be attributed to

restriction and high contact area at support which generated friction between the rollers and the rolling surface. The friction was then transmitted as a resistance force to SCB specimens and manifests itself as increased overall P_{max} in the results.

It can also be noted that visually, roller springs minimally affected how much the test results (i.e., curves) were condensed or spread apart (i.e., band of curves). In addition, all test results ended nearly at approximately the same LPD of 3.5 mm.

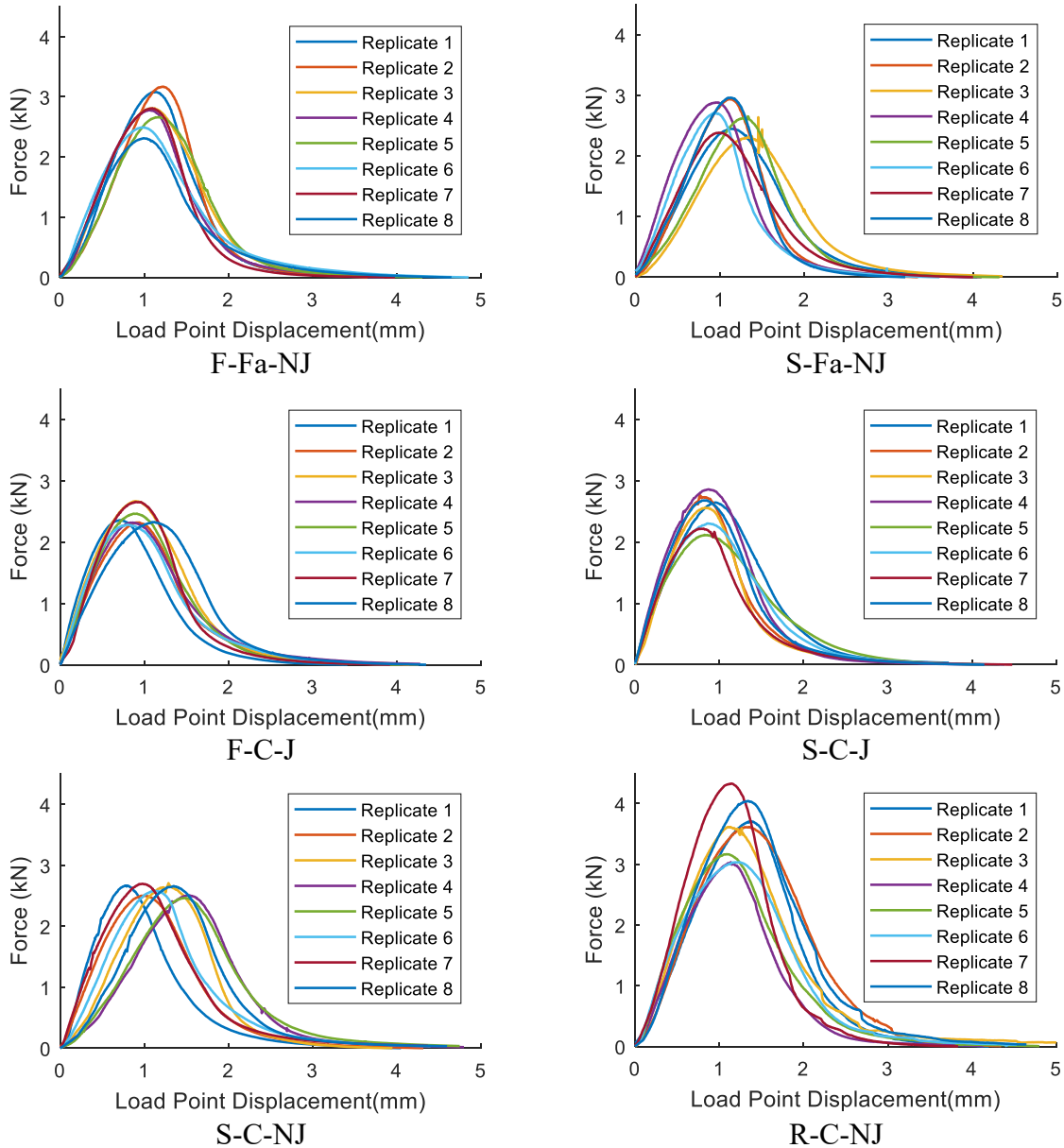


Figure 26. SCB test results (load vs. LPD) of each fixture cases from eight replicates.

Figure 18 shows the averaged force-LPD curve of each fixture case. As aforementioned, the maximum (peak) force of all fixtures appears to be similar except for R-C-NJ which was higher. The average results confirm that roller springs only minimally affected results (force vs. LPD) for both rolling surface shapes (i.e., flat vs. curved) as seen by comparing: F-Fa-NJ vs. S-Fa-NJ and S-C-J vs. F-C-J. For both rolling surfaces, cases without roller springs exhibited a slightly higher peak force. This result implies that the springs reduced the friction at roller supports which is reasonable since the role of springs is to reduce lateral sliding during rolling. It should be noted that increasing the spring constant (i.e., from 0.12 N/mm to higher) on a flat rolling surface would result similar to R-C-NJ. In contrast, decreasing spring constant effectively increased rolling freedom at support result in F-Fa-NJ-like behavior.

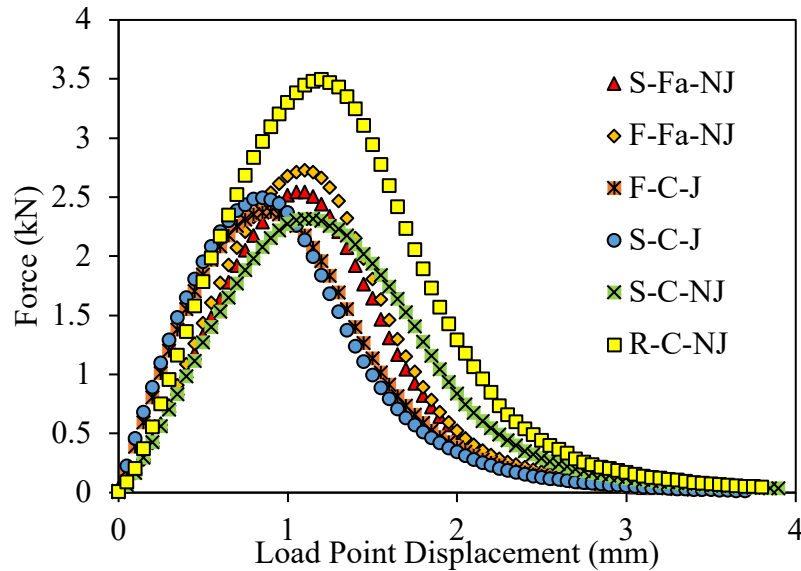


Figure 18. Average per fixture of SCB test results (load vs. LPD).

3.5.6.1 Fracture Energy

Figure 19 present G_f results along with associated COV from all the test fixtures. Results show that R-C-NJ fixture produced the highest G_f among other fixtures which can be attributed to the high work (i.e., area underneath the curve) observed in Figure 18. The jig effect is seen by comparing S-C-J and S-C-NJ. The jig reduced G_f while simultaneously increasing variability (i.e.,

COV). As such, the presence of a jig on an SCB fixture may be detrimental to the repeatability of G_f and thus in case there fracture energy is of interest, the use of jig is not recommended.

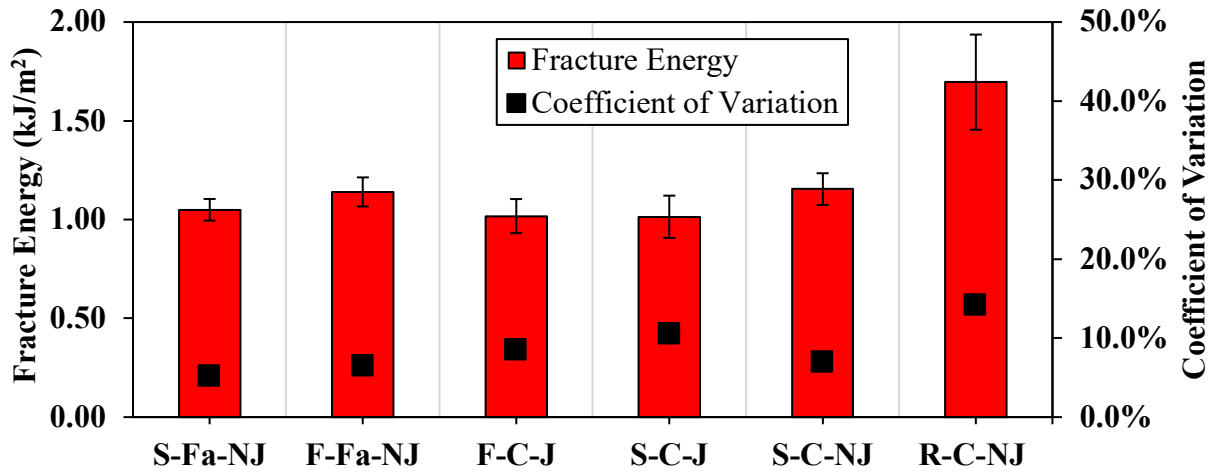


Figure 19. Effect of testing fixtures of fracture energy results and repeatability.

The shape of the rolling surface can be gauged by comparing S-Fa-NJ and S-C-NJ which shows a curved surface increased G_f and COV both by 10%. The effect of roller springs was contrasting for flat and curved rolling surface shapes. On a flat surface, use of springs improved repeatability of G_f while for curved surfaces, they increased COV of G_f . However, it is noted that the springs minimally affected G_f results on both rolling surface shapes. Therefore, the overall recommendation when testing for G_f is to avoid the mid-span jig and use roller springs only on flat rolling surfaces (and avoid them on curved surfaces).

3.5.6.2 Flexibility Index

FI results along with associated COV are shown in Figure 20 and were calculated using Equation 2 from test results of eight replicates per fixtures shown in Figure 26. From the results, the highest FI was obtained from R-C-NJ fixture which is the fixture with restricted curved rolling surface without a mid-span jig. Apparently, the higher G_f translated to higher FI even after normalization of the fracture energy with the post-peak slope (m_2). From the results, it is seen that the presence of the jig (S-C-NJ vs. S-C-J) slightly reduced FI while dramatically increasing COV from 20% to 40%. The jig increases repeatability of FI only when it is used without roller springs (F-C-J vs. S-

C-J). Therefore, when *FI*s of interest, the mid-span jig should only be used without roller springs on a curved surface to improve repeatability of results.

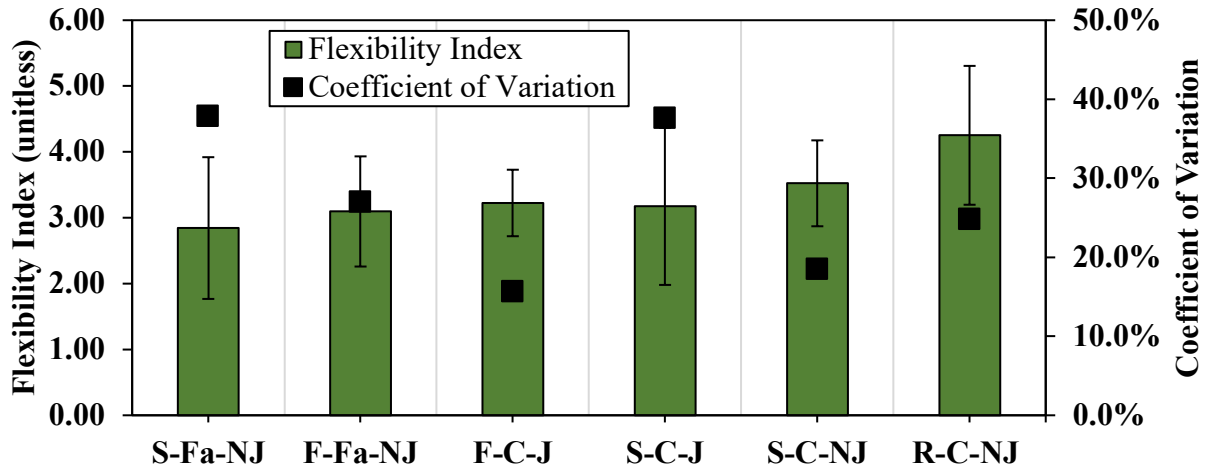


Figure 20. Effect of testing fixtures on flexibility index results and repeatability.

In general, roller springs significantly increased COV of *FI* regardless of the rolling surface shape. In fact, for curved surfaces, COV more than doubled when roller springs were added (F-C-J vs. S-C-J). For the flat surfaces, COV increased by about 50% with the addition of roller springs. Comparing S-Fa-NJ and S-C-NJ, it is noticeable that curved rolling surface improved repeatability of *FI* (i.e., lowered COV). In sum, while roller springs minimally affected the values of *FI*, they greatly contributed to increase COV. In addition, the mid-span jig is only beneficial to the repeatability of *FI* when without springs on curved rolling surface.

3.5.6.3 Maximum Load

The maximum load results shown in Figure 21 indicate similar P_{max} for all fixtures with exception R-C-NJ fixture where the horizontal rolling was restricted. COV of P_{max} results were also similarly low (about 10%), indicating higher repeatability of P_{max} when compared to other indicators such as *FI*. It can be noted that the lowest COV was obtained on S-C-NJ suggesting that curved rolling surface increase repeatability of P_{max} .

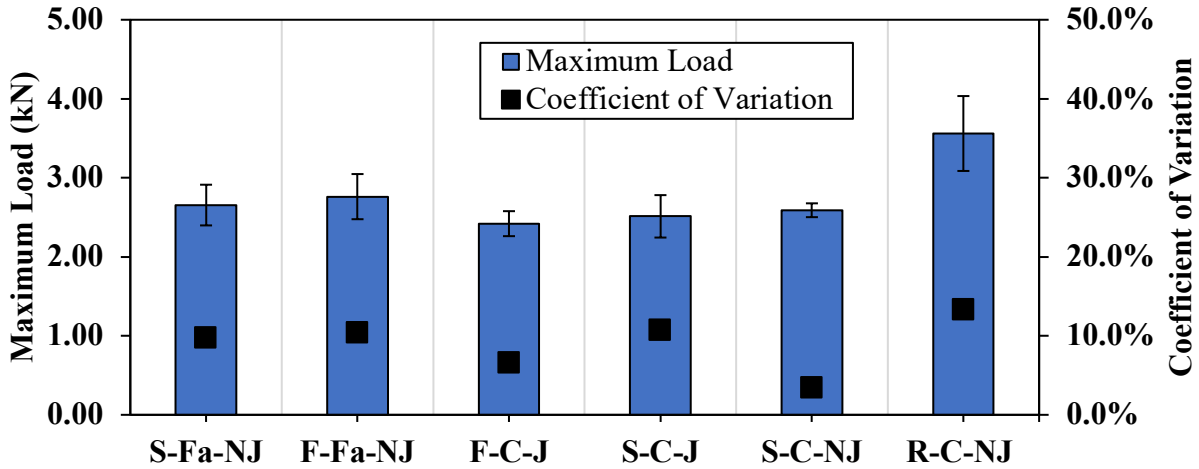


Figure 21. Effect of testing fixtures on maximum load results and repeatability.

3.5.6.4 Cracking Resistance Index

Figure 22 presents *CRI* results calculated from Figure 26 using Equation 3. Error bars considered, *CRI* results from the fixtures were generally similar which is indicative of fixture independency. In addition, the COV results from all fixtures were generally low, around 10%, which suggests high repeatability of *CRI* indicator. The fixture-independence and low COV make *CRI* an attractive indicator to be used when comparing results from different fixtures. However, the lack of sensitivity to the components of the fixture may also be indicative of a lack of power to properly detect an existing difference between mixtures. Thus, more studies on *CRI* sensitivity in AC mixtures are necessary.

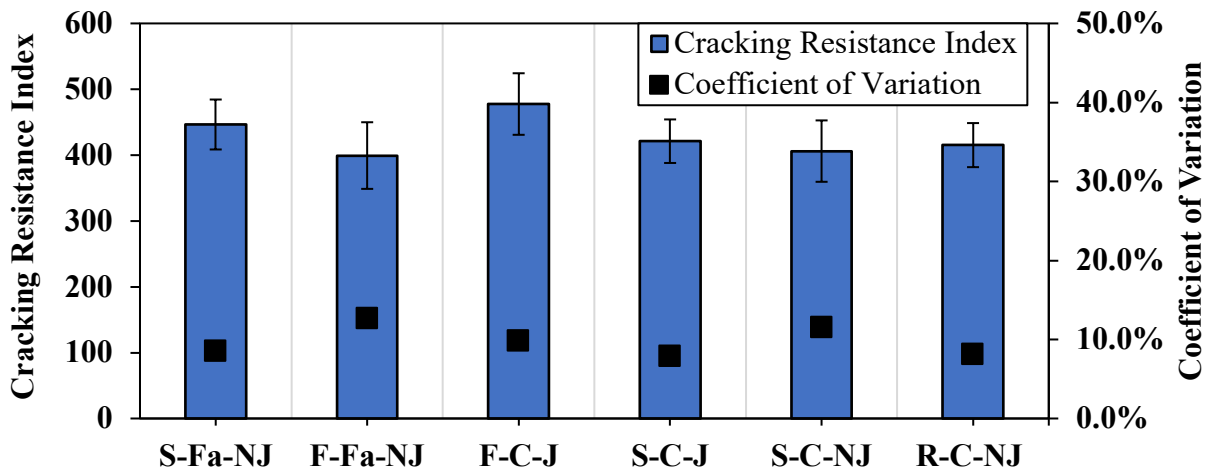


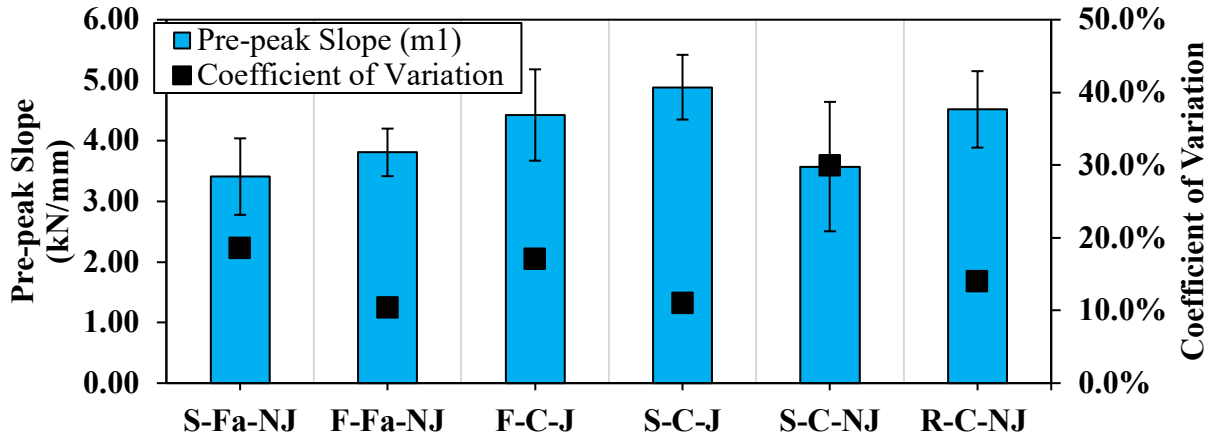
Figure 22. Effect of testing fixtures on cracking resistance index results and repeatability.

3.5.6.5 Pre- and Post-peak Slopes

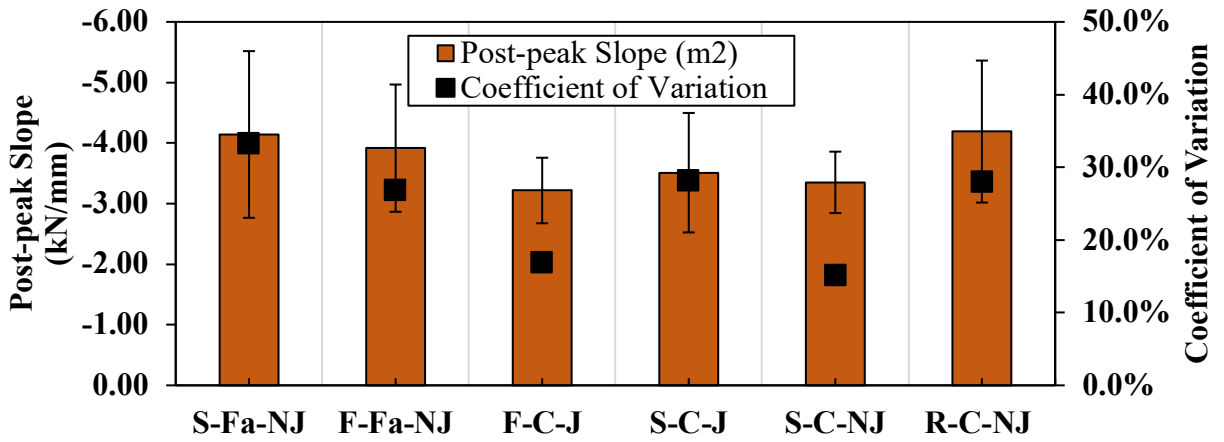
A more fundamental effect of the fixtures on test results can be achieved by examining the characteristics of slopes of the SCB test results curves. Figure 23 shows the slopes of curves: pre-peak (m_1) and post-peak (m_2) in addition to their ratios $\left|\frac{m_1}{m_2}\right|$. The pre-peak slope m_1 can be related to the apparent stiffness of the SCB specimen. Meaning, the higher is m_1 the stiffer is the SCB appears. Figure 23 (a) shows that fixtures with the mid-span jig (F-C-J and S-C-J) had the highest m_1 similar to the fixture with restricted rolling at the support (R-C-NJ). The remaining fixtures had similar m_1 values. COV results indicate that the mid-span jig increased repeatability of m_1 when used with on a curved rolling surface. In addition, roller springs reduced COV on the curved surface (F-C-J vs. S-C-J) while, increasing it on a flat surface.

The post-peak slope m_2 is related to the speed at which SCB fracture is progressing [44]. Results of m_2 are shown in Figure 23 (b) where curved rolling surfaces had lower values compared to flat ones with exception of the fixture with restricted rolling (R-C-NJ). The low m_2 is indicative of reduced crack propagation speed in SCB specimen. COV of m_2 results shows elevated values which are on average double that of m_1 . The increased COV of m_2 has been identified as the main source of the COV of FI results [15, 72]. Repeatability of m_2 can be improved by avoiding a mid-span jig or using the jig on a curved rolling surface.

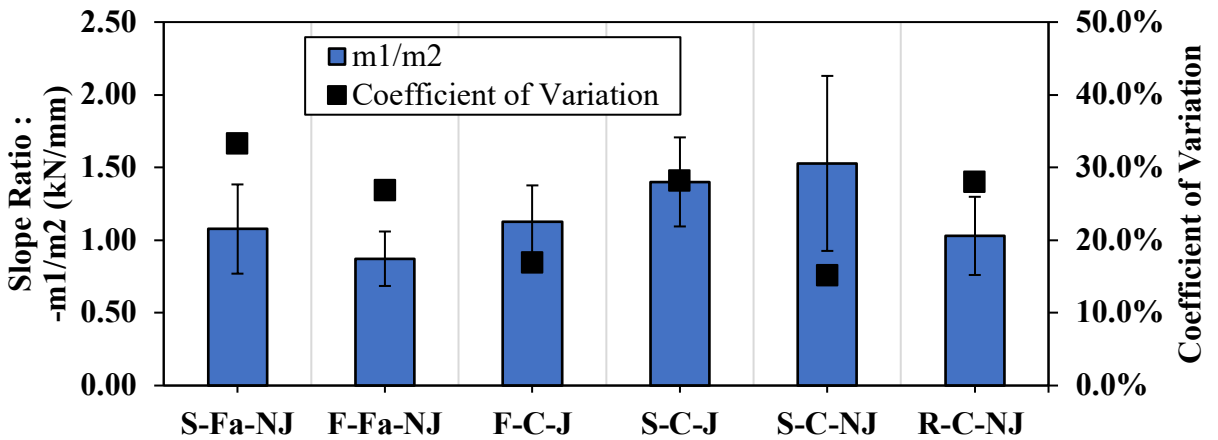
Finally, the slope ratio are compared, and the results are shown in Figure 23 (c). This ratio indicates how fixtures affect the symmetry of the SCB test result curve. If the slope ratio is larger than one, as is the case for both S-C-J and S-C-NJ, then m_1 is higher than m_2 and vice versa. A ratio smaller than one portrays brittle-like behavior of the specimen during testing when the fixture is used. At intermediate test temperature and the loading rate used, the AC mixture is considered compliant. As a result, the fixture which gives a slope ratio lower than one was F-Fa-NJ.



(a)



(b)



(c)

Figure 23. Effect of testing fixtures on slope properties: (a) pre-peak slope, (b) post-peak slope and (c) slope ratios

3.6 Summary

In this chapter, the SCB test method was developed by first investigating critical testing variables such as the recommended minimum number of replicates (n), the thickness of specimens(t), notch length (nl), loading rate(lr), and the testing temperature (T). After the determination of the SCB testing variables based on repeatability and practicality, this chapter also investigated the effects of SCB testing fixtures on the test results and their repeatability. In total six different and prominent testing fixtures were investigated. Table 3 presents the recommended SCB testing variables recommended from test-analysis results.

Table 3. Recommended values for SCB testing variables

Critical Testing Variable	Recommended Value
Number of Replicates	≈ 6
Thickness of Specimen	≈ 50 mm
Notch length	≈ 15 mm
Testing temperature	$\approx 21^{\circ}\text{C}$

The SCB testing fixture investigation revealed that:

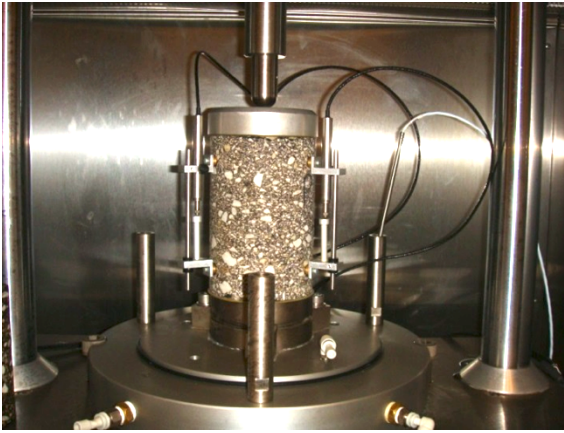
1. Fixtures affected test results, fracture-related indicators, and their associated repeatability
2. When testing for G_f is to avoid the mid-span jig and use roller springs only on flat rolling surfaces (and avoid them on curved surfaces).
3. In general, the mid-span jig should be avoided to improve the repeatability of from SCB test results.
4. While roller springs minimally affected the values of FI , they greatly contributed to the increase of its COV. In addition, the mid-span jig is only beneficial to the repeatability of FI when used without springs and on a curved rolling surface.
5. The fixture-independence and low COV make CRI an attractive indicator for comparing results from different fixtures.

Chapter 4 Rutting Performance Test Method

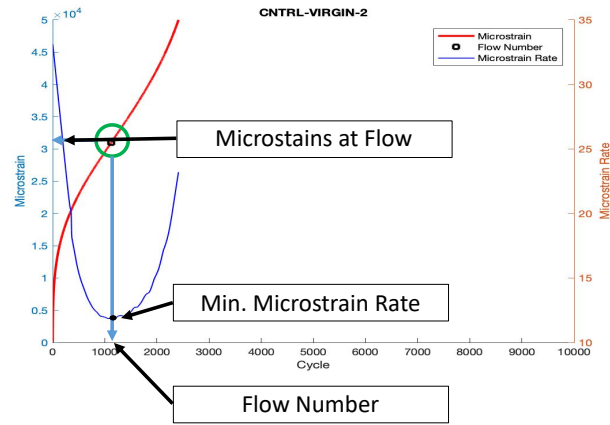
This chapter presents efforts for the development of a simple and practical rutting test called G-Stability. The first part of the chapter focuses on identifying critical testing parameters for the test such as temperature, loading rate, specimen geometry, and a number of replicates. The second part shows a relationship by the correlation between the developed G-Stability test and an existing flow number (FN) rutting test.

4.1 Introduction

Although there are several existing rutting tests, they are usually complicated and require complex equipment to conduct. As aforementioned, among the rutting tests, the FN test has demonstrated a good correlation with field rutting performance [20, 21]. FN is cyclic testing on a cylindrical specimen of 100 mm diameter and 150 mm in height (Figure 24(a)). The specimen is prepared by cutting and coring the SGC tall sample (150 mm diameter and 170 mm height). The cyclic load is applied with 0.1 seconds loading and 0.9 seconds of unloading periods resulting in one second per cycle. The test requires determination of testing parameters such as testing temperature, contact stress, and deviatoric stress to ensure that the flow will occur within 10,000 cycles (i.e., 2 hours 48 minutes). Choosing these testing parameters is time-consuming. It is noted that the test automatically terminates at 50,000 microstrains. Typical test results and data analysis are shown in Figure 24(b) where the flow number is obtained by finding the minimum of a numerically differentiated accumulated microstrains with respect to loading cycles (by first fitting a function to the curve). It is apparent that despite the advantages of FN such as good correlation with field performance, complex testing, and data analysis impedes the testing practicality and wider implementation for BMD. It is thus beneficial to use a more practical, simpler, and sensitive rutting test that is capable of detecting differences in mixtures and presents a good correlation with field rutting performance towards the wider implementation of BMD.



(a)



(b)

Figure 24. Flow number test: (a) set-up and (b) data analysis

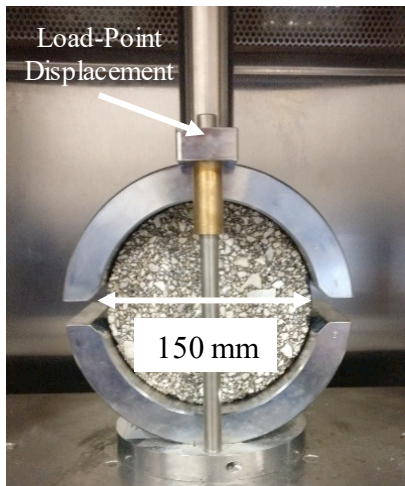
4.2 G-Stability (Gyratory Stability) Test Development

The need to accelerate BMD of Nebraska AC mixtures and lack of practical rutting test motivated this study with the following specific objectives: 1) develop a practical and simple rutting test method, 2) explore the sensitivity of the new rutting test to the difference in mixtures, and 3) validate the developed test method by correlating it to established rutting test (i.e., FN). The new rutting test was named G-Stability after the Superpave gyratory compactor was used to prepare the specimens by measuring stability.

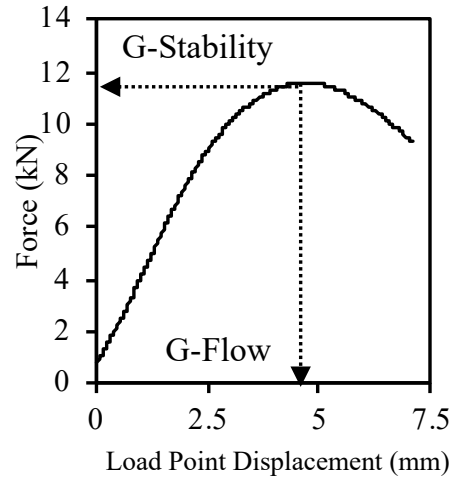
4.2.1 *G-Stability Test Set-up*

The set-up for the G-Stability test is shown in Figure 34(a) and is composed of a disc-shaped AC specimen of 150 mm in diameter loaded using the Marshall stability test fixture. The loading is applied in a displacement-controlled mode. Test results recorded as force and displacement are shown in Figure 34(b). From the results, data analysis is straight forward to determine rutting-related indicators. For example, the maximum load is the “stability”, and the displacement corresponding to the stability is the “flow”.

The advantage of G-Stability rests on simple monotonic displacement-controlled loading which can be performed in most AC laboratories without complicated equipment. Also, the testing fixture (Marshall stability fixture) is widely available in the AC laboratories. In addition, data analysis is extremely simple and can easily be performed visually without complex calculations such as is the case for the FN test.



(a)



(b)

Figure 34. Gyratory stability test: (a) set-up and (b) results and data analysis.

4.2.2 Sample fabrication

The sample fabrication process began with the collection of a mixture from the plant which was then transported in sealed containers to the testing laboratory. The mixture was compacted at recommended compaction temperature using the SGC into tall samples of 150 mm diameter and 170 mm height as shown in Figure 25(a). Subsequently, the tall samples were sliced into discs at the desired thickness. The sample fabrication of G-Stability was considerably simpler than FN since only cutting was needed after compaction, while FN requires coring.



(a)



(b)

Figure 25. SCB sample preparation: (a) compaction by SGC and (b) slicing.

4.2.3 Methodology

The effort to develop G-Stability was subdivided into two phases: 1) development of G-Stability test method, and 2) correlation of G-Stability to FN test. In the first phase, critical testing parameters: temperature (T), loading rate (lr), specimen thickness (t) and number of replicates (n), were determined based on sensitivity, practicality and repeatability. In the second phase, the developed G-Stability and the established FN tests were used to assess the rutting potential of several Nebraska mixtures. Both tests were correlated to each other to investigate the compatibility between the two test methods, which can lead to a relationship between FN and G-Stability. This can improved the validity of the G-Stability method as FN has shown a good correlation with field rutting performance [20, 21]. Figure 36 shows the adopted methodology for the G-Stability test development and comparison with the FN test.

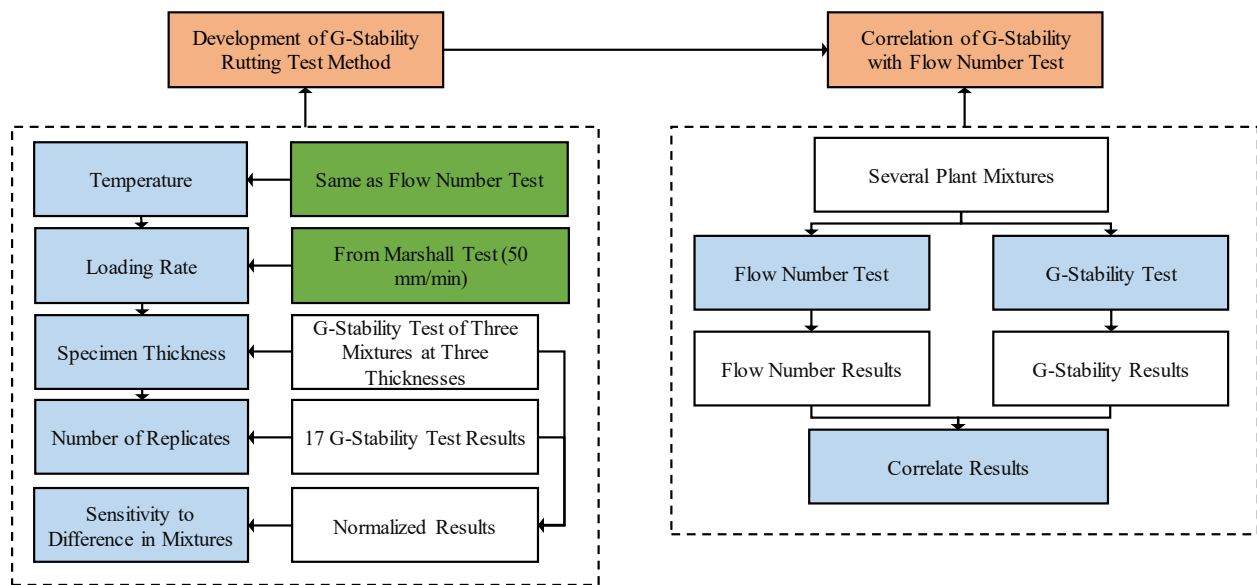


Figure 36. Research methodology for G-Stability showing phases of development and correlation with FN.

4.2.4 Materials

Three AC mixtures were collected over the State of Nebraska and brought to the laboratory in sealed containers to avoid aging by oxidation. The selection of mixtures was made to represent typical mixtures and their usage across Nebraska. The first mixture (Mixture 1) is low-quality mixtures which is mainly used on shoulders or road with very low expected traffic. In addition,

the mixture contained around 50% RAP which is considered a high RAP [44]. The RAP in Mixture 1 is typically sourced from low-quality batches such as those from shoulder pavements. Mixture 1 contained the lowest quality binder (i.e., PG 52-34) among the rests, and the binder content was the lowest (i.e., 5.2%) of all mixtures as shown in Table 4.

The second mixture (Mixture-2) is mainly used as a surface mixture on medium to high traffic roads. The RAP used in Mixture 2 was 45% per weight of the whole mixture and was sourced from better-quality batches than those of Mixture 1. Mixture 2 was designed with 5.3% binder (PG 64-34) and aggregates (nominal maximum aggregate size of 12.5 mm).

Table 4. Key Characteristics of Mixtures Used in Here

Mixture ID	Mixture Name	Usage	RAP	Binder Type and Content (%)
Mixture 1	SPS	Shoulder	50%	PG 52-34 (5.2%)
Mixture 2	SPR	Highway	45%	PG 64-34 (5.3%)
Mixture 3	SLX	Interstate	25%	PG 64-34 (5.4%)

The third mixture (Mixture-3) is considered in Nebraska to be the overall highest quality and has been used for high-traffic roads such as the interstate. Mixture-3, also known as SLX (Table 4), was engineered by the Nebraska DOT to be durable when used as a thin-lift wearing course [36]. The mixture used higher binder content (i.e., 5.4%) than Mixture-2 of the same high-quality binder (PG 64-34) with a lower amount of RAP (e.g., 25%) obtained from good sources. Since the main application of Mixture-3 is for thinner layers, it contains finer aggregates. Table 4 presents the important characteristics of each mixture selected for G-Stability test development. Figure 26 compares the aggregate gradations of the three mixtures.

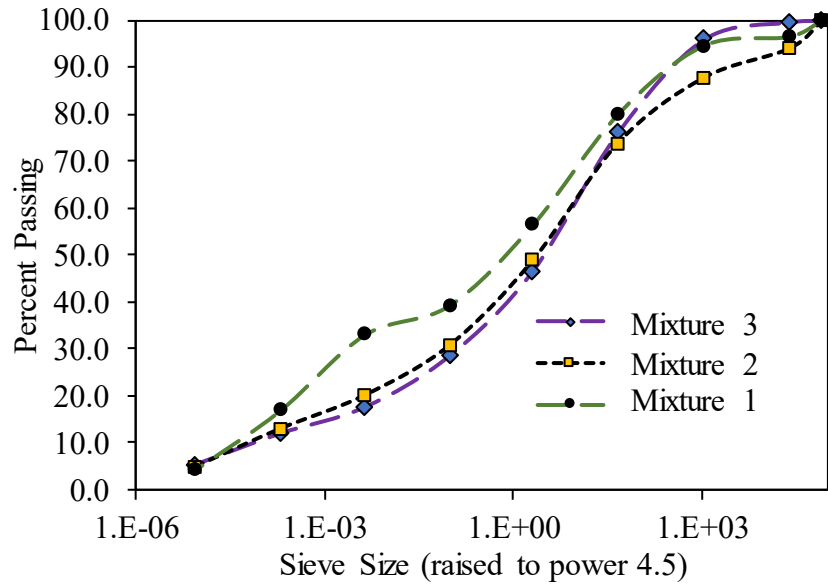


Figure 26. Aggregate gradation of mixtures used in G-Stability development.

4.2.5 Results and Discussions

4.2.5.1 Temperature

It is a well-known fact that rutting usually occurs at high temperatures, the stiffness of AC mixtures is reduced, thus rendering the mixtures susceptible to rutting. For this reason, rutting tests are conducted at high temperatures typically above 40°C [45]. With temperature as a starting point, a preliminary study was conducted to investigate a proper testing temperature using the flow number test. This approach of using an established rutting to infer temperature for G-Stability ensured future compatibility between the two tests. The determination of testing parameters (e.g., contact and cyclic stresses) for the FN test was done according to the recommendation by the AASHTO T 378. First, a combination of temperature, contact stress, and cyclic stress was determined to ensure flow within 10,000 cycles [15]. After multiple trial-and-errors, the temperature of 54°C achieved the reasonable flow using 600 kPa cyclic load and 32 kPa contact stress. As a result, the temperature of 54°C was chosen for the G-Stability rutting test method as well.

4.2.5.2 Loading Rate

To ensure simplicity and practicality of G-Stability, it is critical to the loading rate be readily and easily be achieved in most laboratories without expensive equipment. Towards that, a common loading rate of 50 mm/min corresponding to the widely available Marshall stability test equipment

was adopted for the G-Stability test method. It can help facilitate the implementation of the G-stability test for DOT-friendly BMD practice without requiring expensive-complicated equipment. In addition, G-Stability testing can be achieved without an expensive environmental chamber attached to the test equipment as is the case for the FN test. This is because the fast loading rate of G-Stability allows for the specimen to be tested fast (e.g., within 6 seconds) which can avoid a noticeable temperature drop during testing. The temperature conditioning of G-Stability specimens can easily be achieved by simply using an oven that is available in any AC laboratories. Most notably, G-Stability can reduce testing time significantly compared to others such as the FN, Hamburg, and APA which require at least several hours.

4.2.5.3 Specimens Thickness

Several studies have demonstrated that test results from AC mixtures are thickness-dependent up until saturation thickness from which additional thickness does not improve the accuracy of the results [59, 60, 66]. The saturation thickness is related to the RVE (representative volume element) and is typically four times the NMAS (nominal maximum aggregate size).

Using the predetermined temperature (54°C) and loading rate (50 mm/min), Mixture 1 and Mixture 2 were tested at different thicknesses as shown in Figure 38. The results reasonably show that stability (i.e., maximum load) generally increased with specimen thickness.

The purpose of investigating multiple thicknesses and mixtures was to gauge the expected maximum load for common Nebraska mixtures and select a reasonable specimen thickness that practically satisfies the RVE requirements. Typical loading frames (e.g., AutoSCB™) present in AC laboratories have a maximum capacity of 15 kN or less. As a result, the expected maximum load should not exceed 15 kN to ensure compatibility with the testing frames at most state DOTs and industry laboratories. Based on the results shown in Figure 38, a thickness of 50 mm seems a reasonable geometry, as the maximum loads from both mixtures (high and low quality) were below the 15 kN limit.

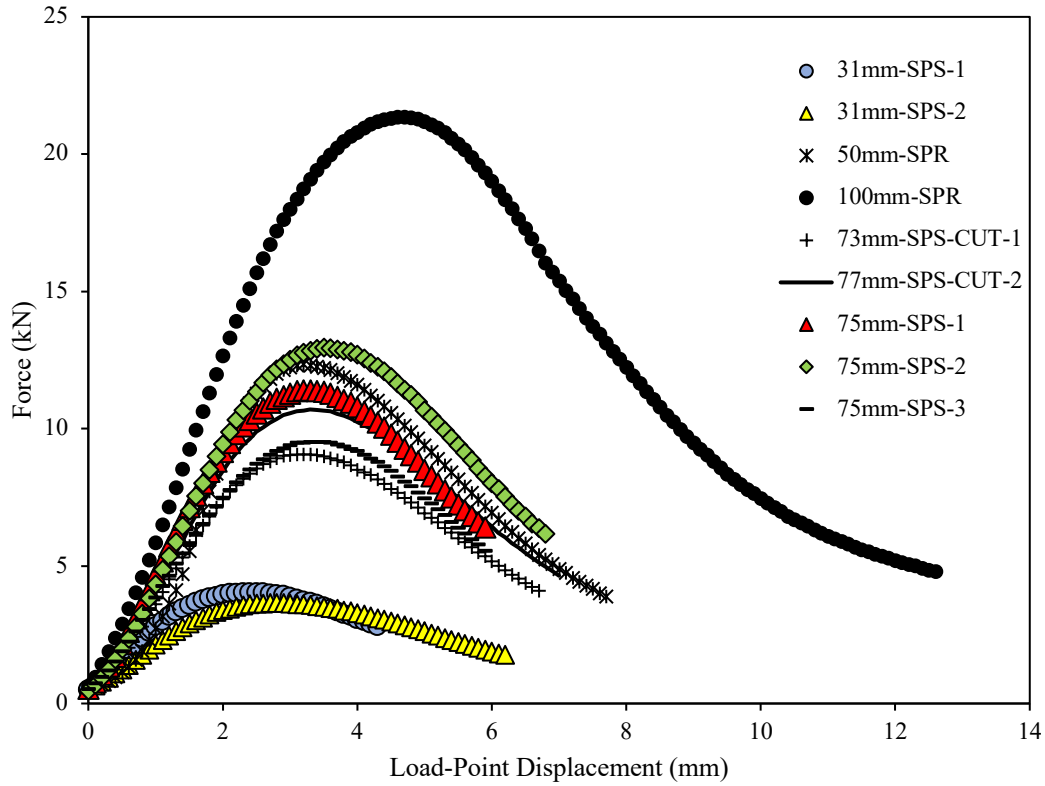


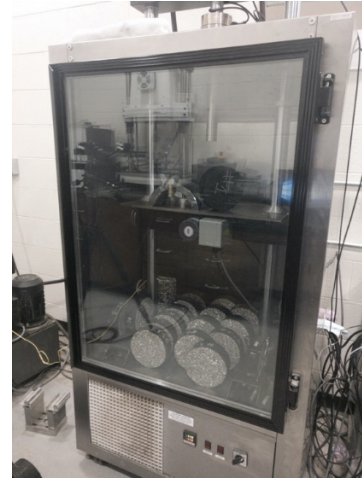
Figure 38. G-Stability testing results at different specimen thickness and mixture.

4.2.5.4 Recommended Minimum Number of Specimens

A total of 17 specimens were prepared from Mixture 3 with other testing parameters determined: the thickness of 50 mm, the temperature of 54°C, and the loading rate of 50mm/min. To determine a recommended minimum number of specimens/replicates, the same process as used in 3.4.3.1 was deployed [73]. Figure 27(a) shows the 17 specimens tested to identify the standard deviation of the population within a desired margin of error.



(a)



(b)

Figure 27. Determination of number of replicates: (a) sample fabrication and (b) environmental conditioning prior testing.

After the environmental conditioning of the test sample (Figure 27(b)), the G-Stability testing was conducted at the aforementioned testing parameters. The testing was conducted on the same day and within the same hour to minimize any other undesired variability. The test results of all 17 specimens are shown in Figure 28. In general, a good repeatability was observed as the difference between minimum and maximum stability was only 3 kN. The average stability was 10.8 kN and its COV was 7.7%, which is indicative of a high repeatability.

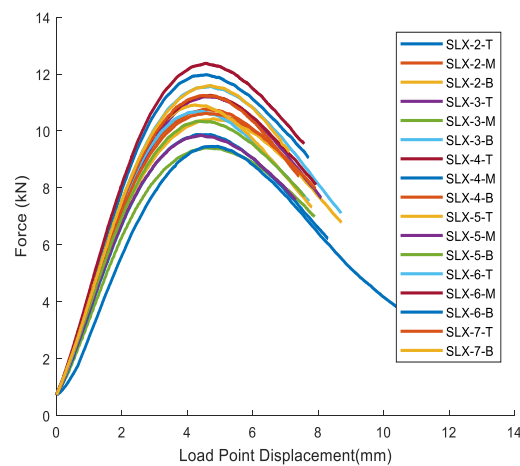


Figure 28. G-Stability test results for minimum replicates determination.

After testing, the Equation 4 was then used to statistically calculate the recommended number of replicates necessary to estimate the mean of the population given a margin of error and a statistical significance (α value). Figure 29 presents the relationship between the margin of error and the minimum number of replicates. It is noted that the curve in Figure 29 was calculated using Equation 4 where a standard deviation ($\sigma = 0.82$ kN) and the standard normal deviate (Z-value) of 1.96 (i.e., $\alpha/2 = 2.5\%$) were used. As the figure presents, more replicates are required to achieve smaller margins of error.

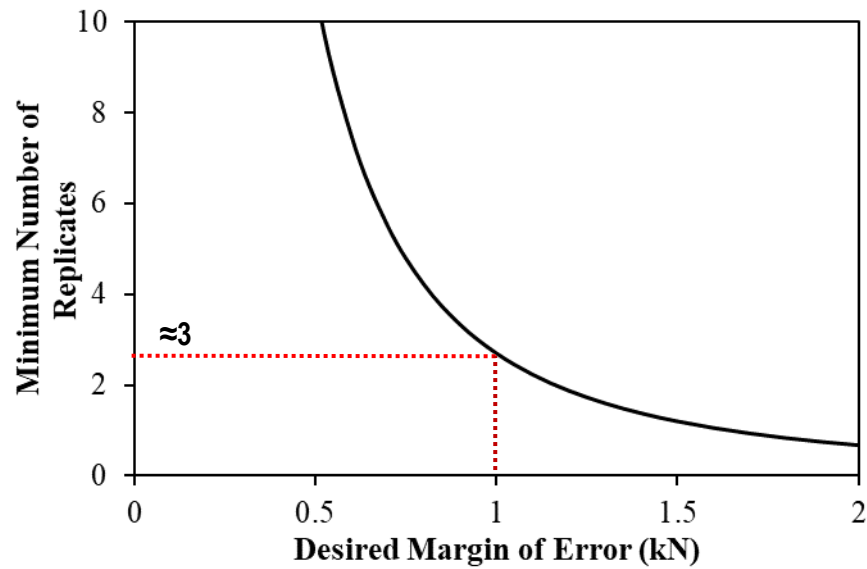


Figure 29. Relationship between the margin of error and the minimum number of G-Stability replicates.

Taking a margin of error of 1.0 kN, the corresponding number of replicates is 3 specimens. Three replicates for G-Stability are particularly attractive as only one tall SGC sample (170 mm high) would suffice to obtain three replicates (50-mm each). This indicates that BMD can be conducted by fabricating two SGC tall samples: one for SCB (six replicates) testing and another for G-Stability (three replicates) testing.

4.2.5.5 Sensitivity of G-Stability

G-Stability test needs to have the capability to detect differences in mixtures as it can be potentially used for mixture design and QA/QC. Therefore, a sensitivity study was conducted on the three mixtures using G-Stability. The sensitivity was checked by comparing test results normalized to thickness as shown in Figure 42 where a difference in results is observed between the AC mixtures. The lowest quality mixture (i.e., Mixture 1) had the lowest stability, while the others (i.e., Mixtures 2 and 3) which were better quality, showed higher peak loads. It can also be noted that, although Mixture 2 and 3 had a similar stability, flow value was different between them. Mixture 3 which is the highest quality mixture tested in here, experienced an enhanced deformation (i.e., higher flow) than Mixture 2. Although more investigation is necessary, the difference in flow values between the two mixtures can be related to the increased performance of Mixture 3. Given both distinction of mixtures in stability and flow values, the G-Stability rutting performance test explored in this project is expected to be a viable method for Nebraska BMD.

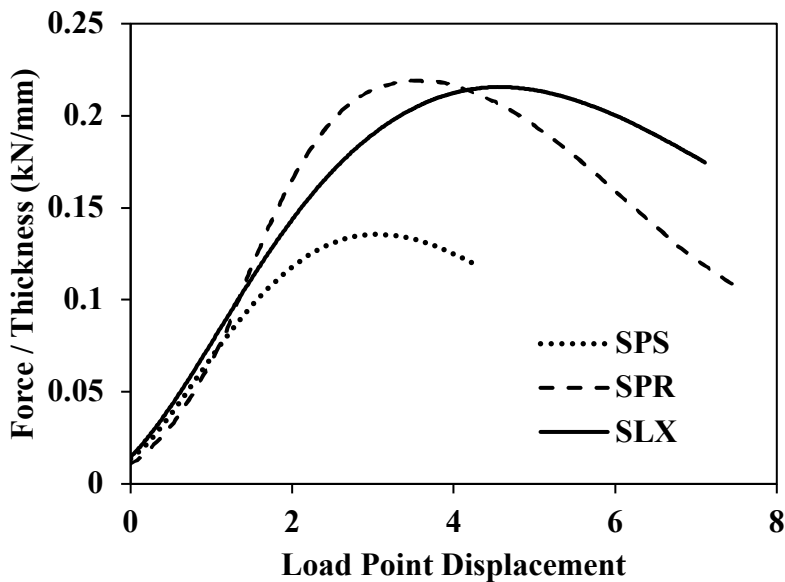


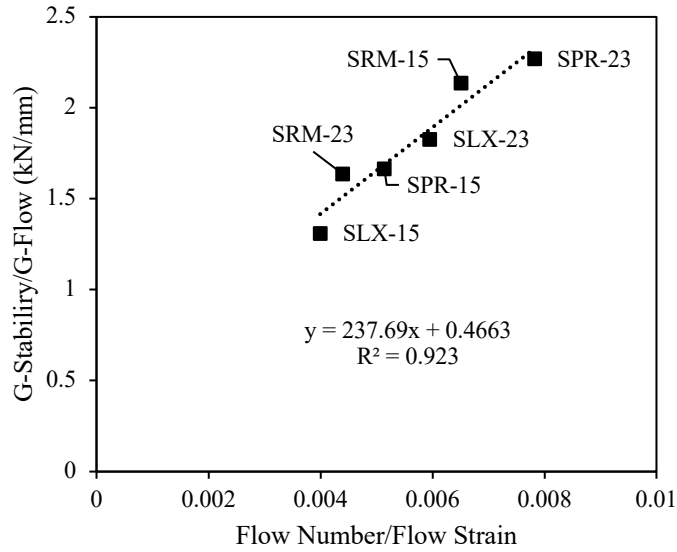
Figure 42. The Sensitivity of the G-Stability Testing Method.

4.3 Correlation of G-Stability to Flow Number Test

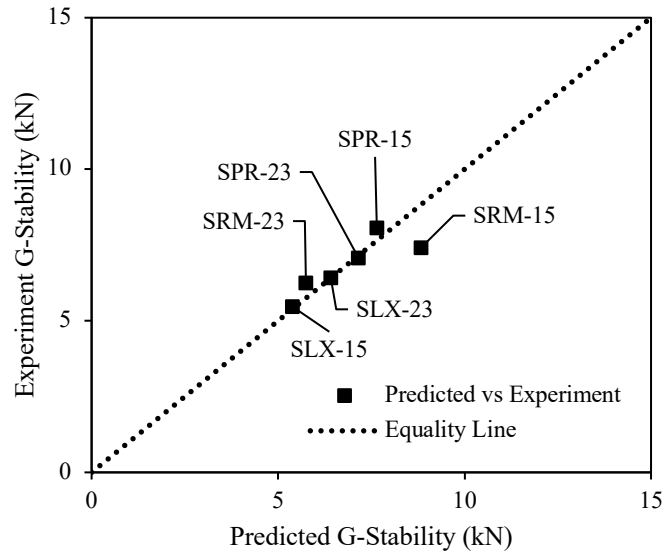
A correlation effort was conducted to establish compatibility between the G-Stability and the FN test results as shown in Table 5. Towards that, several different plant-produced mixtures were collected across the state of Nebraska and were tested for their G-Stability and FN results. A relationship between both data sets was sought. After removing an outlier (Figure 43a), a good correlation was found between the ratio (stability/flow) from G-Stability testing and the ratio (flow number/flow strain) from FN testing as shown in Figure 43(b). The correlation measure of R^2 (coefficient of determination) was 92% which indicates a good correlation between the two test methods.

Table 5. Testing Results Used in Correlation of G-Stability to Flow Number

Indicator	Replicate	SLX-15	SPR-15	SRM-15	SLX-23	SPR-23	SRM-23
G-Stability (kN)	Replicate 1	6.06	8.61	6.61	6.53	6.95	6.31
	Replicate 2	5.08	8.90	7.62	6.01	7.19	6.14
	Replicate 3	5.29	6.72	8.02	6.77	7.15	6.35
	Average	5.48	8.08	7.42	6.44	7.10	6.27
	COV	0.09	0.15	0.10	0.06	0.02	0.02
G-Flow (mm)	Replicate 1	4.44	4.01	3.36	3.93	3.75	3.91
	Replicate 2	4.30	3.71	3.25	3.88	4.24	3.78
	Replicate 3	4.23	3.99	3.44	4.15	3.95	4.18
	Average	4.32	3.90	3.35	3.99	3.98	3.96
	COV	0.02	0.04	0.03	0.04	0.06	0.05
Flow Number	Replicate 1	67.00	75.00	74.00	88.00	90.00	66.00
	Replicate 2	58.00	72.00	97.00	76.00	90.00	66.00
	Replicate 3	56.00	68.00	74.00	64.00	90.00	66.00
	Average	60.33	71.67	81.67	76.00	90.00	66.00
	COV	0.10	0.05	0.16	0.16	0.00	0.00
Flow Strains	Replicate 1	14974.00	9613.00	10167.00	15617.00	15107.00	14988.00
	Replicate 2	15099.00	12218.00	10998.00	14411.00	15107.00	66.00
	Replicate 3	15240.00	11197.00	10149.00	13205.00	15107.00	66.00
	Average	15104.33	11009.33	10438.00	14411.00	15107.00	5040.00
	COV	0.01	0.12	0.05	0.08	0.00	1.71



(a)



(b)

Figure 43. Correlation between G-Stability vs. FN test results: (a) with the outlier and (b) without the outlier

After confirming a good correlation between FN and G-Stability, a comparison study was conducted between the actual experimental results and predicted values. The equation of the linear relationship between the two ratios shown in Figure 43(b) was used to predict G-Stability from FN results as such:

$$\frac{G_{Stability}}{G_{Flow}} = 237.69 \frac{F_{Number}}{F_{Strain}} + 0.4663 \quad \text{Equation 5}$$

where $G_{Stability}$, G_{Flow} , F_{Number} and F_{Strain} are the stability from G-Stability, flow from G-Stability, flow number from FN, and flow strain from FN, respectively.

By taking the flow of 3.92 mm which is the average from all G-Stability test herein, Equation 5 becomes as follows:

$$G_{Stability} = 902.77 \frac{F_{Number}}{F_{Strain}} + 1.77 \tag{Equation 6}$$

Using Equation 6, stability was then predicted, and the results are shown in Figure 30 which is an equality graph. The predicted and actual experimental results were reasonably close to the line of equality which indicates a good prediction capability of Equation 6. This implies that the proposed G-Stability testing and FN testing are interconvertible.

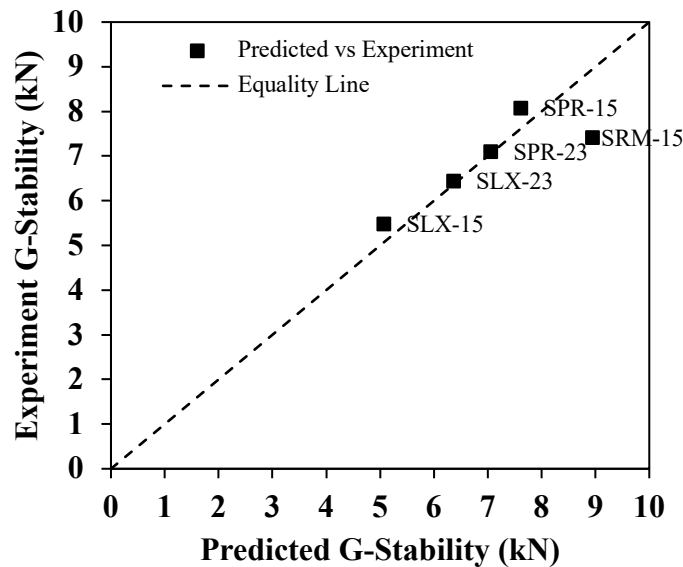


Figure 30. G-Stability predicted from FN vs. experimental results.

4.4 Summary

In this chapter, the G-Stability test which simple, practical, and easy rutting test was explored and correlated to an existing flow number test. Critical testing parameters for the G-Stability test were determined based on repeatability and practicality. The test parameters were temperature, loading rate, specimen thickness, and the recommended minimum number of replicates. Also, sensitivity analysis of the G-Stability test to the existing difference in mixtures was investigated by testing different mixtures and comparing the results. Finally, the correlation study was conducted to gauge

the interconvertibility between G-Stability and FN test by using several Nebraska mixtures from different locations.

In summary, the G-Stability test was efficient to conduct, sensitive to mixtures, and well-correlated with a sophisticated rutting test (FN). G-Stability can be conducted using a typical economic loading frame that can be easily implemented in DOT laboratories. The same loading frame can also be used for the SCB fracture testing which is another performance test to evaluate the cracking potential of AC mixtures. Only two tall SGC samples are necessary to complete both tests, which can potentially accelerate the implementation of BMD in Nebraska.

Chapter 5 Performance Space Diagram (PSD) of Nebraska Mixtures

This chapter uses the mixture test results to examine the feasibility of BMD implementation in Nebraska by using the performance space diagram (PSD). This chapter also presents a plan in which PSD will continuously be enriched by adding mixtures and monitoring field performance.

5.1 Performance Space Diagram

PSD is an important tool for BMD implementation as it allows graphical representation of mixtures according to their fracture and rutting performance test results. The graph, therefore, becomes a two-dimensional representation of a mixture that can help engineers judge mixture performance. A common practice for PSD is to plot fracture-related indicators on the y-axis (vertical) and the rutting indicator in the x-axis (horizontal). A mixture of testing results for both rutting and fracture is then used as coordinates on the graph as exemplified in Figure 31 for typical Nebraska mixtures in Nsengiyumva, Kim [74].

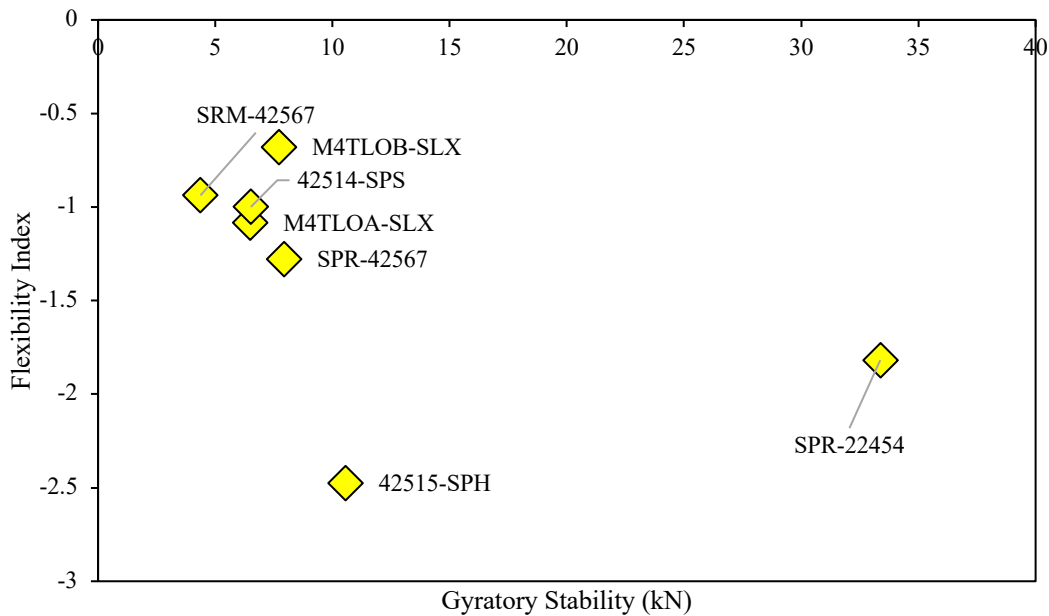


Figure 31. Performance space diagram of typical Nebraska mixtures in Nsengiyumva, Kim [74].

Figure 46 shows a PSD for mixtures used in the correlation of G-Stability to FN. As shown, the PSD relates a cracking indicator (SCB flexibility index) with a rutting indicator (G-Stability). In the figure, mixtures that end with 15 contained RAP sourced from better quality stockpile than mixtures ending with 23. The results show that the quality of RAP does affect mixture performance both in terms of fracture and rutting. It should be noted that only the RAP source was different for mixtures with the same name (e.g., SLX-15 vs. SLX-23). Except for SLX where only fracture performance was improved, the better RAP improved both fracture (*FI*) and rutting performance of mixtures, thus care should be taken when selecting RAP source for mixture design purposes. It demonstrates the strength of BMD which can detect the significance of component properties (e.g., quality of RAP) in mixtures, which is not true in the Superpave volumetric mixture design method.

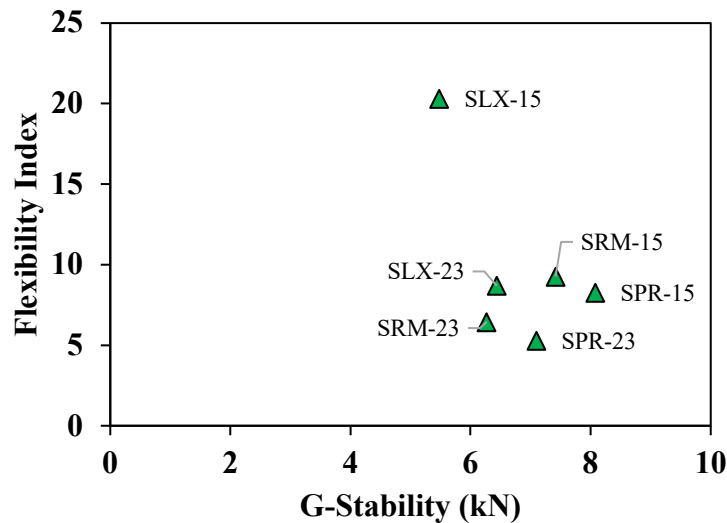


Figure 46. Effect of quality of RAP on PSD of mixtures: better-quality RAP-15 and poor-quality RAP-23.

5.2 Short-term Performance Criteria

As aforementioned, key components of the performance-based mixture design method are the performance tests and performance criteria. Both fracture and rutting need to have criteria, which will serve a threshold to determine whether the performance of a mixture against the distresses is acceptable. The normal method to determine the criteria is to deploy the mixtures in the field and monitor their performance during service. Subsequently, the performance of mixtures in the field is measured using traditional methods such as IRI (international roughness index), visual ranking,

and automatic ranking [75]. The pavement engineer determines which mixtures and corresponding performance-related results that are acceptable [41].

Since G-Stability is a newly developed test, there is a lack of field performance data to determine appropriate performance criteria. However, for the FN test, NCHRP Report 673 by Jenks, Jencks [76] recommended traffic level-dependent rutting performance criteria based on field validation data. As the FN results are interconvertible into G-Stability results using the Equation 6, it is possible to infer rutting performance criteria of AC mixtures based on G-Stability results. It should be noted that this is a short-term way to supplement long-term field performance monitoring, which would require a significant amount of time to complete and out of the scope of this study. Nonetheless, field performance monitoring is underway on several pavement sections in Nebraska and the results can be used to establish the long-term performance criteria of the AC mixtures. Table 3 shows the FN rutting performance criteria per traffic level recommended by the NCHRP report 673 [76]. The FN criteria were then converted into G-Stability to establish performance criteria in terms of G-Stability.

Table 3 Performance Criteria for Rutting in FN and G-Stability

Traffic Level (Million of ESALs)	Minimum Flow Number Requirement*	G-Stability (kN)**
<3	---	---
3 to <10	53	5.55
10 to <30	190	17.24
≥ 30	740	64.17

* recommended criteria from NCHRP report 673, page 142 (AAT, 2011)

** converted from the FN results (using Equation 6)

The other criterion that needs to be determined is for the cracking performance in terms of FI. Similar to the G-Stability rutting criterion, long-term pavement performance monitoring data is needed to practically determine the cracking criterion. However, as the field data require a significant amount of time and cost, this study used the literature where SCB cracking criteria were investigated. Using the literature serves to establish a starting point (i.e., preliminary) while waiting for inputs from the long-term pavement performance. It is of utmost importance to mention

that different AC mixtures require different performance criteria. It is necessary to ultimately establish the performance criteria considering unique mixtures' characteristics, local conditions, and applications. For the FI, a threshold range of five to six is commonly accepted to distinguish poor to acceptable performance of mixtures [77, 78] with exception of the Illinois DOT which uses a threshold of eight [79]. In this study, the preliminary FI limit of six was selected.

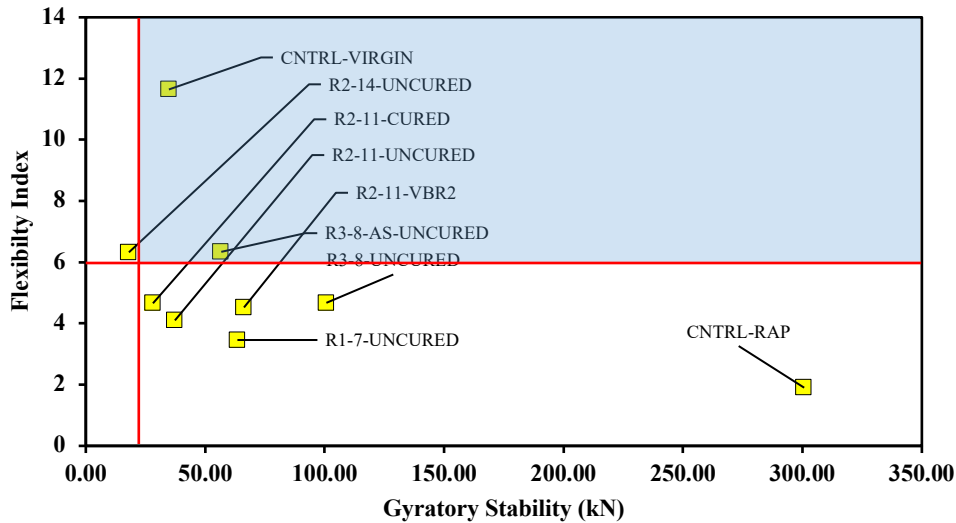


Figure 32. PSD of high-RAP mixtures with performance criteria.

Figure 32 shows the performance space diagram with performance criteria. For the rutting, a criterion of 17.24 kN G-Stability was selected to correspond to the traffic level of 10 to 30 million ESALs. Similarly, other levels of traffic can be selected for PSD from Table 3. The fracture criterion as FI was six. As the PSD shows, according to the performance criteria and the traffic levels used, two mixtures (one high-RAP mixture: R3-AS-UNCURED and the virgin mixture: CNTRL-VIRGIN) satisfied the threshold. This highlights the importance of a performance-based mixture design of high-RAP and the effects of rejuvenators and other additives. Although the performance criteria need adjustment pending field monitoring results, the preliminary criteria can provide help designers improve their mixtures by targeting the blue-shaded corner in Figure 32 that represents a satisfactory performance of mixtures in both rutting and cracking.

5.3 Long-term Performance Criteria

Figure 48 shows the overall concept of PSD that can be used and enriched for Nebraska BMD using the criteria shown in Table 3. The passing zones for typical mixtures (in yellow) and high-RAP mixtures (in blue) are highlighted. This preliminary PSD can be enhanced by adding more mixture performance data and parallel monitoring of long-term field performance for the mixtures. This way will better identify pass/fail limits of Nebraska mixtures to meet satisfactory performance in both cracking and rutting, while the mixtures can be designed more economically.

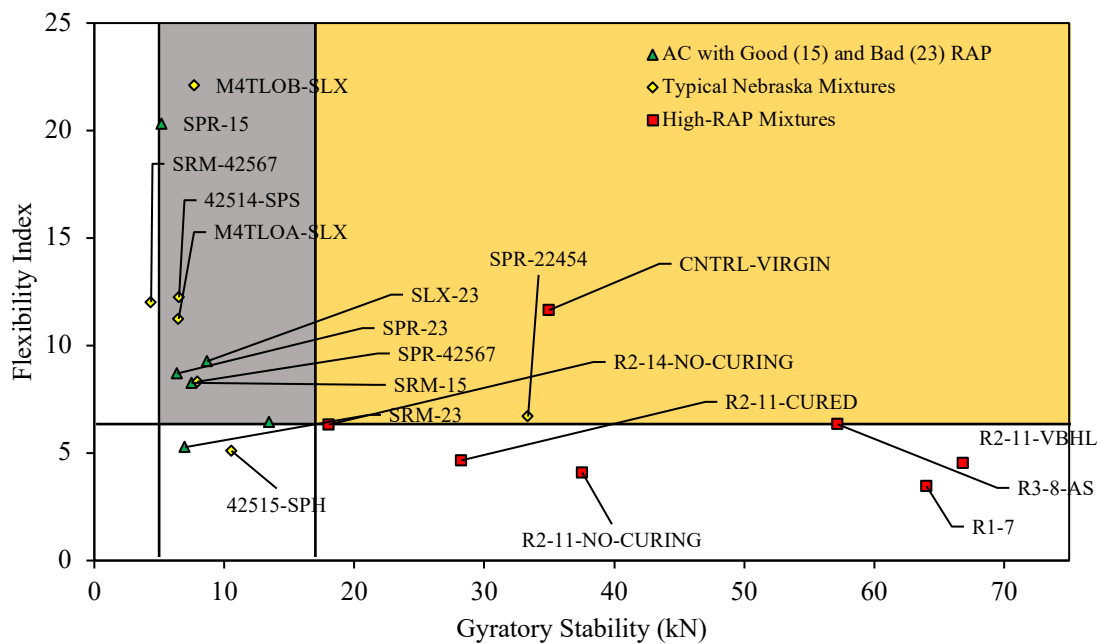


Figure 48. PSD of all mixtures tested here showing the criteria in Table 3 and FI of 6.

Chapter 6 Summary and Conclusions

This study investigated the feasibility of the BMD implementation in Nebraska by systematically developing performance tests for fracture and rutting of AC mixtures. SCB geometry was selected to develop the fracture test method by determining critical testing parameters such as the minimum recommended number of specimens (n), specimen thickness (t), notch length (nl), loading rate (lr), and the testing temperature (T). In addition, SCB testing configurations were also investigated for their effects on test results and their repeatability. For rutting test method development, G-Stability testing was explored, and the testing parameters to provide repeatable and sensitive results were identified. Test results were correlated to the established rutting test of flow number (FN). Finally, both test methods (SCB and G-Stability) were used to construct a performance space diagram in which performance test results of typical Nebraska AC mixtures and some high-RAP mixtures were placed. Based on the test results from this study, the following conclusions can be drawn.

- SCB testing can be conducted in a repeatable manner by testing 5~6 replicates that are at least thicker than 40 mm and possess a notch length greater than 15 but less than 25 mm. The recommended testing loading rate and temperature are 1~3 mm/min and 23°C (room temperature), respectively.
- In general, SCB tests under the fixture conditions examined in this study showed repeatable results, while load-support fixtures affect test results and their repeatability. Friction at the support should be avoided because it can erroneously increase fracture resistance with higher variability. The mid-span jig with roller springs increased testing repeatability.
- G-Stability rutting test was successfully developed and correlated well with established FN test results. G-Stability can be conducted in a repeatable and practical manner by having three 50 mm-thick specimens, tested at 54°C using a 50 mm/min loading rate. G-Stability testing was much simpler to conduct in comparison to FN testing, while test results showed good sensitivity to differentiate AC rutting characteristics.
- A short-term BMD performance threshold was sought using preliminary results from AC mixtures tested in this study. Long-term field performance data should be obtained to more accurately identify the BMD performance criteria in both cracking and rutting.

- Recommended future work includes (1) correlation between SCB and Ideal-CT test results as both tests are conducted at similar testing temperatures and research results from Ideal-CT appear to correlate well with field performance; (2) more mixture data to validate the interconvertibility between G-Stability and FN; (3) a long-term monitoring of field performance to identify Nebraska specific BMD pass/fail criteria; (4) inclusion of low temperature testing and corresponding performance criterion in the Nebraska BMD method for a more comprehensive mixture design practice.

References

1. Zhou, F., et al., *High RAP mixes design methodology with balanced performance*. 2011, United States. Federal Highway Administration.
2. Zhou, F., S. Hu, and T. Scullion, *Integrated asphalt (overlay) mixture design, balancing rutting and cracking requirements*. 2006, Texas Transportation Institute, Texas A & M University System.
3. Haghshenas, H., et al., *Research on high-rap asphalt mixtures with rejuvenators and WMA additives*. 2016.
4. Daniel, J.S. and A. Lachance, *Mechanistic and Volumetric Properties of Asphalt Mixtures with Recycled Asphalt Pavement*. Transportation Research Record, 2005. **1929**(1): p. 28-36.
5. Al-Qadi, I.L., et al., *Testing protocols to ensure performance of high asphalt binder replacement mixes using RAP and RAS*. 2015, Illinois Center for Transportation/Illinois Department of Transportation.
6. Nsengiyumva, G., *Development of semi-circular bending (SCB) fracture test for bituminous mixtures*. 2015.
7. Apeageyi, A.K., *Laboratory evaluation of antioxidants for asphalt binders*. Construction and Building Materials, 2011. **25**(1): p. 47-53.
8. Goodrich, J.L. *Asphalt and polymer modified Asphalt properties related to the performance of Asphalt concrete mixes (with discussion)*. in *Association of Asphalt Paving Technologists Proc.* 1988.
9. Nsengiyumva, G.M., et al., *New Mixture Additives for Sustainable Bituminous Pavements*. 2018: Nebraska Transportation Center.
10. Wagoner, M., W.G. Buttlar, and G. Paulino, *Disk-shaped compact tension test for asphalt concrete fracture*. Experimental mechanics, 2005. **45**(3): p. 270-277.
11. Wagoner, M.P., W.G. Buttlar, and G.H. Paulino, *Development of a single-edge notched beam test for asphalt concrete mixtures*. Journal of Testing and Evaluation, 2005. **33**(6): p. 452-460.
12. Nsengiyumva, G., T. You, and Y.-R. Kim, *Experimental-statistical investigation of testing variables of a semicircular bending (SCB) fracture test repeatability for bituminous mixtures*. Journal of Testing and Evaluation, 2017. **45**(5): p. 1691-1701.
13. Zhou, F., et al., *Development of an IDEAL cracking test for asphalt mix design and QC/QA*. Road Materials and Pavement Design, 2017. **18**(sup4): p. 405-427.
14. Nsengiyumva, G., T. You, and Y.-R. Kim, *Experimental-Statistical Investigation of Testing Variables of a Semicircular Bending (SCB) Fracture Test Repeatability for Bituminous Mixtures*. 2016.
15. Haghshenas, H., et al., *Research on High-RAP Asphalt Mixtures with Rejuvenators-Phase II*. 2019.
16. Carpenter, S.H. and W.R. Vavrik, *Repeated triaxial testing during mix design for performance characterization*. Transportation Research Record, 2001. **1767**(1): p. 76-84.
17. Newcomb, D. and F. Zhou, *Balanced Design of Asphalt Mixtures*. 2018, Minnesota. Dept. of Transportation. Research Services & Library.
18. Williams, R.C., et al., *Testing Wisconsin asphalt mixtures for the AASHTO 2002 mechanistic design procedure*. 2007.

19. Witczak, M., T. Pellinen, and M. El-Basyouny, *Pursuit of the simple performance test for asphalt concrete fracture/cracking*. Journal of the Association of Asphalt Paving Technologists, 2002. **71**.
20. Biligiri, K.P., et al., *Rational modeling of tertiary flow for asphalt mixtures*. Transportation Research Record, 2007. **2001**(1): p. 63-72.
21. Dongré, R., J. D'Angelo, and A. Copeland, *Refinement of flow number as determined by asphalt mixture performance tester: Use in routine quality control–quality assurance practice*. Transportation Research Record, 2009. **2127**(1): p. 127-136.
22. Hajj, E.Y., et al., *Index-Based Tests for Performance Engineered Mixture Designs for Asphalt Pavements*. 2019.
23. Chong, K. and M. Kuruppu, *New specimen for fracture toughness determination for rock and other materials*. International Journal of Fracture, 1984. **26**(2): p. R59-R62.
24. Nsengiyumva, G. and Y.-R. Kim, *Effect of Testing Configuration in Semi-Circular Bending Fracture of Asphalt Mixtures: Experiments and Statistical Analyses*. Transportation Research Record, 2019. **2673**(5): p. 320-328.
25. Nsengiyumva, G., et al., *Mechanical-Chemical Characterization of the Effects of Type, Dosage, and Treatment Methods of Rejuvenators in Aged Bituminous Materials*. Transportation Research Record, 2020. **0**(0): p. 0361198120909110.
26. Zhou, F. and T. Scullion, *Overlay tester: A rapid performance related crack resistance test*. Vol. 7. 2005: Texas Transportation Institute, Texas A & M University System.
27. Buttlar, B. *Disk-Shaped Compact Tension Test*. [cited 2020 3/16]; Available from: <http://www.dot.state.mn.us/mnroad/projects/Low%20Temperature%20Cracking/PDF%207s%20&%20Images/Task%20Reports/SCB%20vs%20DCT%20Fracture%20Test.pdf>.
28. Wu, Z., et al., *Fracture resistance characterization of superpave mixtures using the semi-circular bending test*. Journal of ASTM International, 2005. **2**(3): p. 1-15.
29. Arabani, M. and B. Ferdowsi, *Evaluating the semi-circular bending test for HMA mixtures*. 2009.
30. Zhou, F., *Development of an IDEAL Cracking Test for Asphalt Mix Design, Quality Control and Quality Assurance*. NCHRP-IDEA Program Project Final Report, 2019(195).
31. Walubita, L.F., et al., *The overlay tester: a sensitivity study to improve repeatability and minimize variability in the test results*. 2012, Texas Transportation Institute.
32. Rodezno, M.C., R. West, and A. Taylor, *Flow number test and assessment of AASHTO TP 79-13 rutting criteria: Comparison of rutting performance of hot-mix and warm-mix asphalt mixtures*. Transportation Research Record, 2015. **2507**(1): p. 100-107.
33. Fujie Zhou, B.C., Jun Zhang, Sheng Hu, Jon Epps, and Lijun and Sun, *Development and Validation of an Ideal Shear Rutting Test for Asphalt Mix Design and QC/QA*. Journal of the Association of Asphalt Paving Technologists, 2020.
34. Aschenbrenner, T., *Evaluation of Hamburg wheel-tracking device to predict moisture damage in hot-mix asphalt*. Transportation Research Record, 1995. **1492**: p. 193.
35. Nsengiyumva, G., et al., *Mechanical-Chemical Characterization of the Effects of Type, Dosage, and Treatment Methods of Rejuvenators in Aged Bituminous Materials*. Transportation Research Record: p. 0361198120909110.
36. Im, S., et al., *Evaluation of Thin-Lift Overlay Pavement Preservation Practice: Mixture Testing, Pavement Performance, and Lifecycle Cost Analysis*. Journal of Transportation Engineering, Part B: Pavements, 2018. **144**(3): p. 04018037.

37. Cooper III, S.B., et al., *Balanced asphalt mixture design through specification modification: Louisiana's experience*. Transportation Research Record, 2014. **2447**(1): p. 92-100.
38. Kim, M., L.N. Mohammad, and M.A. Elseifi, *Characterization of fracture properties of asphalt mixtures as measured by semicircular bend test and indirect tension test*. Transportation research record, 2012. **2296**(1): p. 115-124.
39. Bahia, H., et al., *Analysis and feasibility of asphalt pavement performance-based specifications for WisDOT*. 2016, Wisconsin. Dept. of Transportation.
40. Li, X.-J. and M. Marasteanu, *Using semi circular bending test to evaluate low temperature fracture resistance for asphalt concrete*. Experimental mechanics, 2010. **50**(7): p. 867-876.
41. Kim, M., et al., *A simplified performance-based specification for asphalt pavements*. Road Materials and Pavement Design, 2015. **16**(sup2): p. 168-196.
42. Buttlar, W.G., et al., *Performance space diagram for the evaluation of high-and low-temperature asphalt mixture performance*. Road Materials and Pavement Design, 2017. **18**(sup1): p. 336-358.
43. Jahangiri, B., et al., *Performance evaluation of asphalt mixtures with reclaimed asphalt pavement and recycled asphalt shingles in Missouri*. Transportation Research Record, 2019. **2673**(2): p. 392-403.
44. Nsengiyumva, G., et al., *Mechanical-Chemical Characterization of the Effects of Type, Dosage, and Treatment Methods of Rejuvenators in Aged Bituminous Materials*. Transportation Research Record, 2020: p. 0361198120909110.
45. West, R., et al., *Development of a framework for balanced mix design*. Project NCHRP, 2018: p. 20-07.
46. West, R., et al., *Development of a framework for balanced mix design*. NCHRP project, 2018: p. 20-07.
47. Dowdy, S., S. Wearden, and D. Chilko, *Statistics for research*. Vol. 512. 2011: John Wiley & Sons.
48. Ozer, H., et al., *Evaluation of I-FIT Results and Machine Variability using MnRoad Test Track Mixtures*. 2017, Illinois Center for Transportation/Illinois Department of Transportation.
49. Kaseer, F., et al., *Development of an index to evaluate the cracking potential of asphalt mixtures using the semi-circular bending test*. Construction and Building Materials, 2018. **167**: p. 286-298.
50. Duan, K., X.-Z. Hu, and F.H. Wittmann, *Thickness effect on fracture energy of cementitious materials*. Cement and concrete research, 2003. **33**(4): p. 499-507.
51. Li, X.J. and M.O. Marasteanu, *Using Semi Circular Bending Test to Evaluate Low Temperature Fracture Resistance for Asphalt Concrete*. Experimental Mechanics, 2009. **50**(7): p. 867-876.
52. European Committee for Standardization, B., Belgium., *Bituminous mixtures—Test methods for hot mix asphalt—Part 44: Crack propagation by semi-circular bending test*. 2010(EN 12697-44: 2010).
53. Biligiri, K.P., S. Said, and H. Hakim, *Asphalt Mixtures' Crack Propagation Assessment using Semi-Circular Bending Tests*. International Journal of Pavement Research and Technology, 2012. **5**(4): p. 209.
54. Im, S., Y.-R. Kim, and H. Ban, *Rate-and Temperature-Dependent Fracture Characteristics of Asphaltic Paving Mixtures*. JOURNAL OF TESTING AND EVALUATION, 2013. **41**(2): p. 257-268.

55. Machiwal, D. and M.K. Jha, *Hydrologic time series analysis: Theory and practice*. 2012: Springer Science & Business Media.
56. Razali, N.M. and Y.B. Wah, *Power comparisons of shapiro-wilk, kolmogorov-smirnov, lilliefors and anderson-darling tests*. Journal of Statistical Modeling and Analytics, 2011. **2**(1): p. 21-33.
57. Wittmann, X. and H. Zhong, *On some experiments to study the influence of size on strength and fracture energy of concrete*. 1996: Aedificatio Verlag.
58. Brühwiler, E., J. Wang, and F.H. Wittmann, *Fracture of AAC as influenced by specimen dimension and moisture*. Journal of Materials in Civil Engineering, 1990. **2**(3): p. 136-146.
59. Kim, Y., J. Lee, and J.E. Lutfi, *Geometrical evaluation and experimental verification to determine representative volume elements of heterogeneous asphalt mixtures*. Journal of Testing and Evaluation, 2010. **38**(6): p. 660-666.
60. Kim, Y.-R., J.E.S. Lutfi, and D.H. Allen, *Determining representative volume elements of asphalt concrete mixtures without damage*. Transportation Research Record, 2009. **2127**(1): p. 52-59.
61. Park, S.W., Y.R. Kim, and R.A. Schapery, *A viscoelastic continuum damage model and its application to uniaxial behavior of asphalt concrete*. Mechanics of materials, 1996. **24**(4): p. 241-255.
62. Kim, Y.R., H.-J. Lee, and D.N. Little, *Fatigue characterization of asphalt concrete using viscoelasticity and continuum damage theory (with discussion)*. Journal of the Association of Asphalt Paving Technologists, 1997. **66**.
63. Song, S.H., G.H. Paulino, and W.G. Buttlar, *A bilinear cohesive zone model tailored for fracture of asphalt concrete considering viscoelastic bulk material*. Engineering Fracture Mechanics, 2006. **73**(18): p. 2829-2848.
64. Monismith, C.L. and K.E. Secor. *Viscoelastic behavior of asphalt concrete pavements*. in *International Conference on the Structural Design of Asphalt Pavements* University of Michigan, Ann Arbor. 1962.
65. Wineman, A.S. and K.R. Rajagopal, *Mechanical response of polymers: an introduction*. 2000: Cambridge university press.
66. Nsengiyumva, G., T. You, and Y.-R. Kim, *Experimental-Statistical Investigation of Testing Variables of a Semicircular Bending (SCB) Fracture Test Repeatability for Bituminous Mixtures*. Journal of Testing and Evaluation, 2016. **45**(5): p. 1691-1701.
67. Im, S., H. Ban, and Y.-R. Kim, *Characterization of mode-I and mode-II fracture properties of fine aggregate matrix using a semicircular specimen geometry*. Construction and Building Materials, 2014. **52**: p. 413-421.
68. Artamendi, I. and H.A. Khalid, *A comparison between beam and semi-circular bending fracture tests for asphalt*. Road Materials and Pavement Design, 2006. **7**(sup1): p. 163-180.
69. Mahmoud, E., et al., *Extended finite-element modelling of asphalt mixtures fracture properties using the semi-circular bending test*. Road Materials and Pavement Design, 2014. **15**(1): p. 153-166.
70. Fakhri, M. and A. Ahmadi, *Evaluation of fracture resistance of asphalt mixes involving steel slag and RAP: Susceptibility to aging level and freeze and thaw cycles*. Construction and Building Materials, 2017. **157**: p. 748-756.
71. Chehab, G.R., *Characterization of asphalt concrete in tension using a viscoelastoplastic model*. 2002.

72. Nsengiyumva, G. and Y.-R. Kim, *Effect of Testing Configuration in Semi-Circular Bending Fracture of Asphalt Mixtures: Experiments and Statistical Analyses*. Transportation Research Record, 2019: p. 0361198119839343.
73. Nsengiyumva, G., *Development of Semi-Circular Bending (SCB) Fracture Test for Bituminous Mixtures*, in *Civil Engineering*. 2015, University of Nebraska-Lincoln: December 2015.
74. Nsengiyumva, G., Y.-R. Kim, and T. You, *Development of a Semicircular Bend (SCB) Test Method for Performance Testing of Nebraska Asphalt Mixtures*. 2015.
75. Rami, K.Z. and Y.-R. Kim, *Nebraska data collection*. 2015, Nebraska Transportation Center.
76. Jenks, C., et al., *NCHRP Report 673: A manual for design of hot mix asphalt with commentary*. Transportation Research Board, Washington, DC, 2011.
77. Ozer, H., et al., *Fracture characterization of asphalt mixtures with high recycled content using Illinois semicircular bending test method and flexibility index*. Transportation Research Record, 2016. **2575**(1): p. 130-137.
78. Batioja-Alvarez, D., J. Lee, and J.E. Haddock, *Understanding the Illinois Flexibility Index Test (I-FIT) using Indiana Asphalt Mixtures*. Transportation Research Record, 2019. **2673**(6): p. 337-346.
79. Ali, U.M., I.L. Al-Qadi, and H. Ozer, *Flexibility Index Threshold Optimization for Various Asphalt Concrete Mixes and Climatic Conditions*. Transportation Research Record, 2020. **2674**(1): p. 104-112.